91602
new 82-10

ontario hydro
research division

COMPLIMENTARY COPY
Please Credit Ontario Hydro Research if
Reproduced in Whole or in Part

OXIDATION AND BIAXIAL DEFORMATION BEHAVIOUR OF CANDU ZIRCALOY-4 FUEL CLADDING IN AIR IN THE TEMPERATURE RANGE 873-1123 K

Report No 87-10-K

E.T.C. Ho - Engineer-Metallurgical
A. Donner - Technologist
Materials Integrity Section
Metallurgical Research Department

ABSTRACT

A test program has been carried out to study the oxidation and biaxial deformation behaviour of CANDU Zircaloy-4 fuel cladding material over the temperature range 873-1123 K, in an air environment. Results obtained indicate that braze heat-affected zone (HAZ) material oxidizes 1.2-2 times more rapidly than parent cladding material. Empirical correlations for the oxidation behaviour of both parent and braze HAZ materials were developed using the test data. For the test conditions examined, the oxidation of both parent and braze HAZ materials was consistent with post-transition or linear kinetic behaviour. The elevated temperature biaxial deformation behaviour was characterized by local ballooning in the weaker parent material at high pressures, and by specimen failures in braze HAZ material at low pressures due to the more rapid oxidation of the latter material. Tentative criteria for embrittlement and handling of CANDU Zircaloy-4 fuel cladding were developed using the experimental oxidation data and the room temperature fracture energy data. Recommendations were made to extend the tensile testing to elevated temperatures and to carry out additional oxidation tests in order that more quantitative criteria for embrittlement and handling may be developed.

job	file	date	report no.
84-237-450	823.22	July 6, 1987	87-10-K

91602
new 82-10

ontario hydro
research division

EXECUTIVE SUMMARY

OXIDATION AND BIAXIAL DEFORMATION BE[illegible]VIOUR OF CANDU ZIRCALOY-4 FUEL CLADDING IN AIR IN THE TEMPERATURE RANGE 873-1123 K

E.T.C. Ho and A. Donner

Objectives: The major objectives of the test program were to generate oxidation kinetic data for CANDU Zircaloy-4 fuel cladding and to develop suitable embrittlement and handling criteria needed in the analysis of postulated accident and fuel handling scenarios in which the cooling for the fuel bundles at low decay power levels has degraded.

Major Results of Study:

1. Over the temperature range 873-1123 K, braze heat-affected zone (HAZ) material oxidizes from 1.2 to 2 times more rapidly than parent material in an air environment. Empirical correlations for the oxidation behaviour were developed using the test data.

2. For the ranges of temperature and time investigated, the oxidation of both parent and braze HAZ materials is consistent with post-transition or linear kinetic behaviour.

3. The elevated temperature biaxial deformation behaviour is characterized by local ballooning in the weaker parent material at high pressure, and by specimen failure in braze HAZ material at low pressures due to its higher oxidation rate.

4. Tentative criteria for embrittlement and handling of CANDU Zircaloy-4 fuel cladding were developed using the experimental oxidation data and the room temperature fracture energy data.

Recommendations:

Tensile testing should be extended to elevated temperatures and additional oxidation tests should be carried out to obtain more quantitative oxidation and materials properties data. Such data are needed to develop more quantitative criteria for embrittlement and handling of CANDU Zircaloy-4 fuel cladding.

job	file	date	report no.
84-237-450	823.22	July 6, 1987	87-10-K

TABLE OF CONTENTS

		Page
1.0	INTRODUCTION	1
2.0	EXPERIMENTAL	1
2.1	Material	1
2.2	Oxidation and Biaxial Deformation Studies	1
2.3	Metallographic Examinations	3
2.4	Mechanical Testing	3
3.0	EXPERIMENTAL RESULTS	3
3.1	Oxidation Behaviour and Kinetics of Parent and Braze HAZ Materials	3
3.2	Biaxial Deformation Behaviour of Partially Oxidized Fuel Cladding	4
3.3	Mechanical Properties of Partially Oxidized Fuel Cladding Material at Room Temperature	4
4.0	REVIEW OF EXISTING EMBRITTLEMENT CRITERIA FOR ZIRCALOY-4 CLADDING	5
5.0	DISCUSSION OF RESULTS	6
5.1	Oxidation Behaviour and Kinetics	6
5.2	Biaxial Deformation Behaviour	7
5.3	Mechanical Properties of As-Received and Oxidized Fuel Cladding Material at Room Temperature	8
6.0	TENTATIVE EMBRITTLEMENT AND HANDLING CRITERIA FOR CANDU ZIRCALOY-4 FUEL CLADDING MATERIAL	9
7.0	CONCLUSIONS	10
8.0	RECOMMENDATIONS	11
	ACKNOWLEDGEMENTS	11
	REFERENCES	13
	TABLES	15
	FIGURES	21
	DISTRIBUTION	last page

ontario hydro
research division

To Dr. G. Brenciaglia
Manager
Fuels and Physics Department

OXIDATION AND BIAXIAL DEFORMATION BEHAVIOUR OF CANDU ZIRCALOY-4 FUEL CLADDING IN AIR IN THE TEMPERATURE RANGE 873-1123 K

1.0 INTRODUCTION

There is a paucity of materials data on the oxidation and deformation behaviour of CANDU reactor Zircaloy-4 (Zr-4) fuel cladding for temperatures in the range 673-1173 K. Apart from the early air oxidation experiments carried out by Wolicky/1/, which were analyzed by Doyle/2/, there is very little information available for assessment of oxidation and embrittlement of Zr-4 fuel cladding for the above-mentioned temperature range. Unfortunately, such data are required in the analysis of a number of post-shutdown accident scenarios and fuel handling incidents in which the fuel bundles at low decay levels are postulated to heat-up due to degraded cooling conditions. To alleviate the above situation, a test program was proposed/3/ to acquire the required materials data. The initial phase of the proposed test program entailed the development of an appropriate test facility. This facility has been developed and it has been described in detail elsewhere/4/. It was anticipated that the test data obtained could be used to develop appropriate embrittlement and "handling" criteria for degraded (partially oxidized and deformed) fuel cladding. The use of such criteria would then permit one to set realistic times which are needed to react safely to the various postulated accident scenarios.

2.0 EXPERIMENTAL

2.1 Material

The material used in the present study was Bruce-sized reactor-grade (ie, meeting all AECL/OH specifications in terms of chemical composition and mechanical properties) Zr-4 fuel cladding. The fuel elements were supplied by Westinghouse Canada Limited. Both CANLUB and non-CANLUB fuel sheathing were supplied and used in the oxidation and biaxial deformation experiments. The fuel cladding had been processed to the "sub-assembly" stage/5/: that is, to the production stage where the bearing and spacer pads have been induction brazed to the fuel cladding.

2.2 Oxidation and Biaxial Deformation Studies

The oxidation and biaxial deformation studies were carried out using the test facility developed specifically for the test program and it has been described in detail elsewhere/4/. Specimen heating was achieved using in-house designed and built resistance tube furnaces. The tube furnaces were deployed in two principal configurations, namely, horizontal and vertical. More

specifically, the vertical set-up was used when the heat-up time, generally 20-40 minutes, was only a small fraction of the total oxidation time. This configuration was amenable to immediate water quenching of the samples following elevated temperature exposure. Otherwise, the horizontal configuration was used. The main advantage of the horizontal configuration was a more rapid approach to and stabilization at the desired hold temperature. Biaxial deformation of test samples was accomplished using FLODAR fittings for pressure sealing the fuel cladding and using argon gas for internal pressurization. Prior to elevated temperature exposure or high temperature deformation, the fuel cladding samples were instrumented with three (3) type-K thermocouples (TC's) which were spot welded to the centre of the sample and 6.35 or 5.08 cm on both sides of the central TC. Platinum pads about 2x2x0.075 mm in dimension were used to prevent interdiffusion between the bare TC beads and the Zr-4 material. Most of the test samples were also gauged with two Pt pads spaced about 12.7 cm apart. These two markers were used for measurement of axial strain associated with the oxidation or biaxial deformation.

The test procedure used to carry out an oxidation test under zero differential pressure was as follows:

1. An appropriately instrumented test specimen was fitted with FLODAR fittings and attached to the stainless steel tube fixture.

2. The specimen and fixture assembly was evacuated and back-filled with argon gas a couple of times and then sealed using a shut-off valve.

3. The specimen and fixture assembly was mounted in the tube furnace which was in most cases in the vertical orientation. This configuration was used for the lower temperature tests in which the heat-up times were only very small fractions of the overall elevated temperature exposure times. For the higher temperature tests, the horizontal configuration was used.

4. The above assembly was heated to prescribed test temperatures and held for a predetermined length of time. During this entire period, the temperatures at the three monitored locations were recorded at preselected time increments.

5. Upon completion of the oxidation time, the hot specimen was quenched by allowing it to plunge into a cylinder filled with tap water.

The test procedure used to carry out elevated temperature biaxial deformation testing was as follows:

1. A test sample fitted with FLODAR fittings was attached to the appropriate fixture and pressure tested by immersing the assembly in an aluminum trough filled with water.

2. The sample was then cleaned, dried, instrumented with three type-K TC's and two Pt pads, installed in the furnace (horizontal configuration) and attached to the pressurizing circuit of the test facility.

3. The pressure circuit was evacuated and back-filled with argon a couple of times and then pressurized to the desired test pressure.

4. Power was applied to the furnace and elapsed time indicator. Slight pressure increases during the temperature ramp to the desired test temperature were manually relieved via metering/shut-off valves installed immediately downstream of the gas regulator.

5. Upon failure of the test piece, a pressure switch performed the following actions: a) de-energizes a solenoid valve which isolated the sample from the pressure source, b) trips a relay to turn power off to the furnace; c) turns power off to the elapsed time indicator.

2.3 Metallographic Examinations

Samples oxidized under essentially zero differential pressure were used to obtain oxidation kinetic data. To achieve this, rings about 5 mm wide were cut from the partially oxidized samples using a lubricated diamond wafer blade saw. A preliminary metallographic investigation showed that the microstructure of the braze HAZ was fairly uniform except for a small region a few millimeters wide (transition zone) adjacent to parent cladding material. Therefore, samples representative of braze heat-affected zone (HAZ) material were removed from the centre of the test piece and samples representative of parent material were removed from about 6.35 cm from the centre position. Both of these locations were within the central monitored zone of the sample. The parent and braze HAZ rings were mounted and polished using standard metallographic practice for zirconium alloys. The polishing plane was normal to the tube axis. Measurements of oxide and remaining wall thickness were obtained from micrographs taken at 100 X or at higher magnifications for the specimens with very thin oxides. Samples for detailed substrate metal microstructural examinations were repolished, etched and anodized. Micrographs of the microstructures were taken using polarized light.

2.4 Mechanical Testing

The mechanical properties of partially oxidized cladding samples were obtained by conducting miniature D-ring tensile tests. The ring samples, about 5 mm wide, were cut from the partially oxidized samples using a lubricated diamond wafer blade saw. A schematic diagram illustrating how the samples were cut is presented in Figure 1. As shown in the figure, only one of the rings is unequivocally representative of braze HAZ material.

The miniature D-ring tensile tests were carried out using a custom-designed test fixture shown in Figure 2 and a computer-controlled servo-hydraulic Materials Characterization Test Facility. The rings were pulled apart under a constant ram speed of 5×10^{-2} mm/s to fracture. For each test, a complete set of load versus ram displacement data was recorded.

3.0 EXPERIMENTAL RESULTS

3.1 Oxidation Behaviour and Kinetics of Parent and Braze HAZ Materials

The appearance of samples oxidized for various times at 873, 923, 973, 1023, 1073 and 1123 K are presented in Figures 3 and 4. As shown in the photographs, the severity of oxide cracking and spalling increases with time at a given temperature. Most of the oxidized samples (oxide thickness >30 μm) exhibited a buff-light brown colour oxide. The thinner oxides (< 10 μm) were black in colour. The transition zone was usually discernible and appeared as a lighter brown colour ring. Data obtained from detailed measurements of oxide and substrate metal thicknesses are presented in Table I and plotted in Figures 5 and 6. The results show clearly that the braze HAZ material oxidizes considerably more rapidly than parent material under comparable

conditions over the range of temperatures investigated. The results also indicate that for the range of times examined at each temperature, the oxidation behaviour is consistent with a linear or post-transition kinetic law.

3.2 Biaxial Deformation Behaviour of Partially Oxidized Fuel Cladding

The appearance of samples deformed under biaxial stress conditions at elevated temperatures in an air environment are shown in Figures 7 and 8. The results show clearly that at relatively high internal pressures, the parent material deforms by expanding or ballooning until the sample ruptures when the remaining tube wall had been reduced sufficiently by a combination of straining and oxidation, with the former being the dominant factor. However, at low internal pressures, the samples invariably fail in braze HAZ material with relatively small diametral expansion. The failure locations were usually at bearing or spacer pad interfacial regions (Figures 8(b) and 8(c)). A plot of rupture time as a function of differential pressure at 973 K is presented in Figure 9. This figure shows that the critical pressure which causes the failure location to switch from parent to braze HAZ material lies in the range 0.6-0.8 MPa at 973 K.

3.3 Mechanical Properties of Partially Oxidized Fuel Cladding Material at Room Temperature

The typical appearances of the load vs ram displacement curves for as-received and various degree of oxidized fuel cladding material are presented in Figures 10-13. The data in Figure 10 are characteristic of as-received cladding material. In general, the parent material has higher yield and tensile strengths than the braze HAZ material. The plots in Figure 11 are typical of slightly oxidized parent and braze HAZ material, with the latter exhibiting an apparent yield phenomenon. After sufficient oxidation, both the parent and braze HAZ materials exhibit apparent yield phenomena, as shown in Figure 12, the plots in Figure 13 show that both the parent and braze HAZ materials are severely embrittled by extensive oxidation. In this seriously embrittled condition, the parent ring failed at loads slightly exceeding yield while the braze HAZ ring failed during elastic loading.

Micrographs of the microstructures of the various types of fuel cladding material represented in Figures 10-13 are presented in Figures 14-17. The microstructure of as-received parent and braze HAZ material consists of very fine but deformed α-Zr grains and very large prior-β Widmanstatten grains, respectively. The micrographs in Figures 15 and 16 indicate that the major effect of the oxidation or elevated temperature exposure on the microstructure of as-received parent material is recrystallization and grain growth to produce a much coarser, equi-axed α grain structure. In comparison, under similar conditions, the Widmanstatten microstructure of the as-received braze HAZ material is changed very little. However, after extensive or severe oxidation (Figure 17), both the parent and braze HAZ remaining metal microstructures exhibit significant deformation after water quenching.

Tables II and III present summaries of all tensile data obtained from the test program. The energy absorbed to fracture was estimated by numerically integrating the load vs ram displacement curve. The energy data presented in Figure 18 and 19 show that the room temperature fracture toughness of oxidized cladding material generally decreases with increasing degree of oxidation.

4.0 REVIEW OF EXISTING EMBRITTLEMENT CRITERIA FOR ZIRCALOY-4 CLADDING

Several embrittlement criteria for oxidized Zr-4 fuel cladding have been proposed/6-9/ in the literature. They all involve refinements to the highly conservative US NRC acceptance criteria/10/ for emergency core cooling systems for light-water cooled reactors under loss-of-coolant accident (LOCA) conditions. The conditions for the above criteria are, (a), the oxidation must be less than 17% of the original wall and, (b), the peak temperature must be less than 1473 K. The more refined embrittlement criteria invariably involve the condition of the substrate metal as the main factor determining embrittlement.

It is well established that, at elevated temperatures, oxygen diffuses readily from the oxide layer into the substrate metal. This diffusion results in the formation of an oxygen-stabilized α-Zr layer beneath the oxide phase. This α-layer is strong but has low fracture toughness (ie, brittle). The flux of oxygen into the substrate metal also increases the strength of the substrate by solid solution strengthening. However, this strength increase is also accompanied by a concomitant reduction in fracture toughness.

Early studies on the embrittlement of Zircaloy by Hobson and Rottenhouse/6,11/ indicated that Zircaloy containing more than 0.7 wt% oxygen was brittle at room temperatures. They also noted that when the saturation of oxygen in the β-Zr phase was greater than 90%, α-incursions were formed which would contribute to embrittlement. After reviewing the data of Hobson and Rittenhouse, Pawel/7/ concluded that the distribution of oxygen in the prior-β phase plays an important role in determining the load-carrying capacity of the cladding. He therefore proposed that Zircaloy is embrittled if the average oxygen concentration in the β-phase is equal or greater than 0.7 wt% and equal or greater than 95% saturation.

Based on data obtained from tensile testing of oxidized Zr-4 cladding samples, which showed that the load-carrying capacity of oxidized samples was confined to the low-oxygen part of the prior-β phase, Sawatzky/8/ proposed an interim embrittlement criterion. Sawatzky's criterion states that "the oxygen concentration must be less than 0.7 wt% over at least half of the cladding thickness".

Chung et al/9/ carried out an extensive materials test program, which included both rupture tests of tube samples and Charpy impact tests of sheet specimens, to develop an appropriate criterion for oxygen embrittlement applicable to LOCA conditions for light water reactors. Their results showed that under thermal shock-loading conditions (ie, bottom-flooding with water at about 290 K), the hot tubes invariably failed when the thickness of the transformed β with less than or equal to 1.0 wt% oxygen was less than or equal to 0.1 mm. In particular, their data showed that for oxidized Zr-4 cladding to fail under thermal shock loading, the material must be in a "brittle" condition at the temperature at which the transition from film to nucleate boiling occurs - namely, the Leidenfrost temperature. Furthermore, Chung et al concluded that a more quantitative criterion, based upon the mechanical behaviour of the oxidized material, can be formulated with a specified degree of conservatism consistent with the mechanical loads imposed on the cladding during reflood. The work of Chung et al showed clearly that to develop more quantitative criteria for embrittlement of Zircaloy, extensive materials data, such as fracture toughness data, are required.

However, for the range of temperatures and times investigated in the present study, the amount of oxygen diffusing into substrate metal is not expected to be a dominant factor, such as the situation under LOCA-type conditions. For the test conditions examined, it is reasonable to

assume that the conditions of the oxide and remaining substrate metal will control the mechanical behaviour of the partially-oxidized cladding material. The nature of this mechanical response will then determine the toughness of the oxidized cladding material.

5.0 DISCUSSION OF RESULTS

5.1 Oxidation Behaviour and Kinetics

Since the principal objective of the oxidation tests was to produce engineering-type data suitable for use in establishing embrittlement and "handling" criteria, only moderately fast heating rates were used. The heat-up times were typically in the range 20-40 min. In the plots presented in Figures 5 and 6, the oxidation times plotted correspond to the total time from the start of temperature ramping from ambient temperature. Therefore, when the total oxidation period is one day or greater, the heat-up time is only a very small fraction of the total exposure time. As a result, the error associated with the use of the total time for the isothermal oxidation period is not very great. However, when the total exposure time is only a few hours, the heat-up times become a significant fraction of the exposure time. Nevertheless, visual inspection of the data presented in Figures 5 and 6 indicate that the individual points of each of the data sets may be fitted quite reasonably using a least-squares line. Consequently, this analysis technique was performed for each data set and the least-squares lines obtained are given in Table IV.

From the above discussion, it is evident that true activation parameters can not be extracted from the oxidation data. In spite of this limitation, we have analyzed the b-parameter (ie, slope) of the least-squares lines, which are representative of the linear reaction rate constants (k_L's), and the results are presented in Table V and Figure 20. The ln k_L vs 1/T plots in Figure 20 indicate that a pseudo activation energy may be obtained for parent and braze HAZ materials. For the temperature range studied, the activation energy obtained for parent and braze HAZ materials are 151 and 137 kJ/mole, respectively. These values are in reasonable agreement with linear oxidation activation energies reported for Zr and Zr-alloys/12-15/.

The oxide thickness vs time plots presented in Figures 5 and 6 indicate that for the range of times investigated at each temperature, the oxidation behaviour of both parent and braze HAZ materials is consistent with a post-transition or linear kinetic law. This observation is consistent with the Zr-4 fuel cladding data presented by Leistikow et al/16/, which showed that the oxidation undergoes a transition to linear kinetics for temperatures in the range 873-1073 K. Incubation times to post-transition behaviour, estimated from the data presented by Leistikow et al, are shown in Figure 21. This plot shows clearly that all the experimental times investigated were well beyond the transition times to linear kinetics.

The oxidation data presented in Figures 5 and 6 show clearly that braze HAZ material oxidizes much more rapidly than parent material for the ranges of time and temperature studied. More specifically, the oxidation rates of braze HAZ material were 1.2-2.0 times faster than parent material. Although the oxidation of both types of material is consistent with linear kinetics, the activation energy for parent material was larger. At the present time, we have no explanation for this difference in oxidation behaviour. However, we note that the microstructure and texture of parent and braze HAZ materials are very different. These factors may be partly responsible for the observed differences in oxidation behaviour.

The least-squares line correlations for the oxidation of parent and braze HAZ materials have been used to construct "life times diagrams" (ie diagram showing time needed to oxidize 100% of wall thickness as a function of temperature) for Zr-4 fuel cladding material, and the results are presented in Figure 22. The current Ontario Hydro embrittlement criterion/17/ for Zr-4 fuel cladding material (based on 40% oxidation of the original wall thickness) is plotted in a similar manner. However, since the experimental data are not pure isothermal oxidation data, the linear rates are underestimated, especially at the upper end of the temperature range examined. In view of the above, a "modified" life times diagram was constructed and is presented in Figure 23. In this diagram, the time needed to reach 40% oxidation were calculated using the oxidation correlations but omitting the constant term in the equations.

The plots of life times vs temperature in Figures 22 and 23 show a rather sharp change in slopes at about 973 K. Since the pseudo linear reaction rate constants do not exhibit such a sharp break, this change must be attributable to other factors. The data in Figure 21 indicate that the incubation time to break-away oxidation exhibits a sharp change at about 973 K. The above observation, together with the fact that as the oxidation temperature was increased the heat-up time becomes a larger fraction of the exposure time, have contributed to produce the sharp change in the life times curves at 973 K.

Comparisons of oxidation data obtained from normal oxidation tests with those obtained from biaxial deformation tests carried out at 973 K indicate that the presence of a hoop stress did not have a significant effect on the oxidation rate. However, more quantitative tests must be carried out at other temperatures before a more definitive statement on the effect of a hoop stress on oxidation kinetics can be made.

Comparisons of the oxidation rate correlation predictions with available literature data for Zr-4 fuel cladding material are presented in Table VI. The results show that the empirical correlation predictions are in very good agreement with data report by Sagat/18/, which were obtained by oxidizing parent Pickering-type Zr-4 fuel cladding material in an air environment. However, the predicted values are in very poor agreement with the oxidation data (in steam) reported by Leistikow et al/16/. The reasons for this poor agreement is not fully understood at present, but some researchers have reported that air is a much more aggressive medium than steam with respect to oxidation at certain temperatures. At a test temperature of 1173 K, Sagat/18/ found that the oxide thickness was about three(3) times greater in air than in steam, after 0.7 h of oxidation.

5.2 Biaxial Deformation Behaviour

When a fuel cladding sample is subjected to an internal pressure at elevated temperatures, the sample will deform by expanding outwards or ballooning. The nature of the deformation is determined by the relative magnitude of the internal pressure, the temperature and the time of exposure. Over the range of temperatures investigated, the deformation behaviour may be divided into three different groups, determined by the relative magnitude of the internal pressure. These pressure conditions are:

a) relatively high pressures;
b) intermediate pressures;
c) relatively low pressures.

The deformation behaviour at relatively high pressures is characterized by substantial ballooning,

principally at the highest temperature regions in parent cladding material. After a sufficient amount of wall thinning due to ballooning, the sample ruptures. Depending on the magnitude of the pressure, this rupture can be in the form of a small axial crack (specimens 2 and 3 in Figure 8(a)) or in the form of a classic cod-mouth rupture (specimens 1 and 2 in Figure 7).

At intermediate pressures, both the straining of parent material and the more rapid oxidation of braze HAZ material play equally important roles in determining the degradation of the fuel cladding and the ultimate failure mode. Within this pressure range, there exists a critical pressure below which failure of the cladding occurs in braze HAZ material. For a test temperature of 973 K, this critical pressure lies in the range 0.6-0.8 MPa. Although we have no experimental data to verify the following hypothesis, it is reasonable to postulate that this critical pressure will decrease as the temperature is increased.

The deformation behaviour at relatively low pressures is determined mainly by the higher oxidation rate of the braze HAZ material. At low pressures, the failures occur invariably in braze HAZ material. In particular, the failure locations were mainly in close proximity to the interfacial regions between cladding and bearing/spacer pads. The failures were in the form of small hairline cracks, as shown in Figures 8(b) and 8(c). The micrographs presented in Figure 24 show clearly that the final rupture occurred in cladding material. Since the failures occur preferentially at the leading or trailing edges of the bearing pads, it is evident that factors other than oxidation per se have played a role in determining this behaviour. The concave shapes of the bearing pads after severe oxidation (Figure 1(a)) suggest that the failure is stress-assisted, and the source of this stress may be residual or differential thermal stresses.

The above described deformation behaviour is illustrated by the results obtained from conducting a series of biaxial tests at 973 K, as shown in Figures 8 and 9. The curve in Figure 9 shows clearly that at low pressure the samples fail invariably in braze HAZ material and that the extrapolation to failure time at zero differential pressure is not linear.

5.3 Mechanical Properties of As-Received and Oxidized Fuel Cladding Material at Room Temperature

As noted in Section 4.0 the development of more quantitative criteria for embrittlement of Zr-4 fuel cladding requires extensive materials data. To obtain some of the required information, miniature D-ring tensile tests were carried out using as-received and various degree of oxidized fuel cladding materials. Summaries of the tensile results are shown in Tables II and III. In describing the mechanical behaviour of the various materials tested, we have divided the materials into four different types, and they are as follows:

(a) as-received material;
(b) mildly oxidized material;
(c) intermediately oxidized material;
(d) severely oxidized material.

The tensile properties of parent and braze HAZ materials are quite different in the as-received condition (Table II). The parent material has significantly higher yield and tensile strengths. In addition, the ratio of yield to tensile strengths is about 0.9 for parent material compared to about 0.75 for braze HAZ material. The latter ratio value is characteristic of a material with isotropic tensile properties. These observations are consistent with the level of cold work and the texture

developed in production Zr-4 fuel cladding and with the known effects of the braze cycle on the parent material. The tensile data also show that the energy absorbed to fracture, which is a measure of the fracture toughness of the material, is significantly higher in parent material. This higher toughness can probably be traced to the fine grain size of the parent material (Figure 14).

The mechanical behaviour of mildly oxidized (few % oxidation) material is illustrated by the load vs ram displacement curves presented in Figure 11. The yield and tensile strengths of parent material have decreased due to recovery, recrystallization and grain growth processes. In contrast, the yield and tensile strength of braze HAZ material have increased. These increases can probably be attributed to oxygen-strengthening and/or second phase particle strengthening. In this condition, both types of materials have similar values for the energy absorbed to fracture and these values are still relatively high so that the materials still have good fracture toughness.

The mechanical behaviour of intermediately oxidized (few %-35%) material is illustrated by the load vs ram displacement curves in Figure 12. The yield and tensile strengths of parent material have increased relative to their values in the mildly oxidized condition. These increases may be attributed to oxygen-strengthening and/or particle strengthening. In contrast, the yield and tensile strengths of braze HAZ materials have increased only slightly from their values in the mildly oxidized state. However, the toughness of the braze HAZ material has degraded noticeably from that of the mildly oxidized condition. In this intermediately oxidized stage, the fracture toughness of both parent and braze HAZ materials generally decreases with increasing degree of oxidation.

The mechanical behaviour of severely oxidized (>35%) material is shown by the data presented in Figure 13. In this condition, both the parent and HAZ materials have low fracture toughness. The severely oxidized ring samples fail during elastic loading or slightly into yield. Such behaviour was observed when the material had oxidized in excess of about 50% of the original wall, although some exceptions were observed. The absorbed energy to fracture for delineating such behaviour is about 2×10^5 J/m^2. Below this value, low fracture toughness was invariably observed, although a few cases of low fracture toughness were observed at absorbed energies greater than the above figure.

In summary, it appears that the energy to fracture is a better measure of the toughness of the oxidized cladding than is the amount of oxide growth, for oxidation in the temperature range 873-1123 K. The experimental data showed clearly that the mechanical behaviour of samples with similar oxide thicknesses, but grown under different temperatures, can be quite varied (Figure 18 and 19).

6.0 TENTATIVE EMBRITTLEMENT AND HANDLING CRITERIA FOR CANDU ZIRCALOY-4 FUEL CLADDING MATERIAL

As noted in the Introduction, one of the main objectives of the present study was to establish suitable criteria for embrittlement and handling of oxidized Zr-4 fuel cladding material. Results obtained from tensile testing indicate that both parent and braze HAZ oxidized materials exhibit low toughness when the energy absorbed to fracture was 2×10^5 J/m^2 or less. Therefore, using this somewhat arbitrary energy value as the embrittlement criterion and utilizing the data presented in Figures 18 and 19, the times to reach this embrittlement condition at a given temperature may be calculated using the oxide growth correlations presented in Table IV. The results obtained are presented in Figure 25.

Detailed analysis of the fracture energy data indicate that the samples failed at low loads (ie, during elastic loading or slightly into yield) when the energy was less than about 1×10^5 J/m^2. If we now assume that this energy is the lower limit for handling oxidized fuel cladding, then data for the handling criterion may be obtained using the same procedure as that used for the embrittlement criterion. The data obtained are also presented in Figure 25.

By performing least-squares analyses of the above data, the following linear relationships for embrittlement and handling of parent and braze HAZ materials were found.

1. Embrittlement criterion:

   (a) parent material $y = 7.91 - 6.37 \times 10^{-3} x$;
   (b) braze HAZ material $y = 8.27 - 6.86 \times 10^{-3} x$,

2. Handling criterion:

   (a) parent material $y = 8.14 - 6.51 \times 10^{-3} x$;
   (b) braze HAZ material $y = 8.16 = 6.69 \times 10^{-3} x$.

In the above equations, $y = \log t$, where t is the time in hours and x is the temperature in°K.

From the above discussion, it is evident that if more quantitative or definitive criteria for embrittlement and handling are to be established, additional tests must be carried out.

7.0 CONCLUSIONS

1. Over the temperature range 873-1123 K, braze HAZ material oxidizes from 1.2 to 2 times more rapidly than parent material, in an air environment.

2. From the analyses of the oxidation data, empirical correlations for the isothermal oxide growth rates of both parent and braze HAZ materials were developed.

3. For the ranges of temperature and time studied, the oxidation of both parent and braze HAZ materials is consistent with linear reaction rate kinetics.

4. Analysis of the pseudo-linear reaction rate constants for parent and braze HAZ materials produce activation energies of 151 and 137 kJ/mole, respectively. These values are somewhat higher than linear activation energies reported for Zr and Zr-alloys in the literature. This observation is consistent with the fact that the pseudo-linear rate constants underestimate the true rate constants.

5. Comparison of the parent material oxidation data with literature data indicates that oxidation in an air environment is more rapid than in a steam environment.

6. At any given temperature, the biaxial deformation behaviour may be summarized as follows:

   (a) at relatively high pressures, the samples fail by ballooning to rupture in parent material and the degradation in fuel cladding properties is strain-dominated;

(b) at intermediate pressures, both the ballooning of parent material and the more rapid oxidation of braze HAZ material play equally important roles in determining the ultimate failure mode;

(c) at relatively low pressures, the samples fail invariably in braze HAZ material and the degradation in fuel cladding properties is oxidation - dominated.

7. From analysis of the room temperature tensile data, tentative criteria for embrittlement and handling, based on the value of the absorbed energy to fracture, were developed.

8. Results obtained from the elevated temperature biaxial tests and the room temperature tensile tests indicate that the yield and tensile strengths of as-received parent material decrease rapidly at elevated temperature due to recovery, recrystallization and grain growth processes.

8.0 RECOMMENDATIONS

1. Mechanical testing of oxidized samples should be extended to elevated temperatures to increase the data base for CANDU Zr-4 fuel cladding material. Such data are needed to develop more quantitative criteria for embrittlement and handling.

2. Additional tests should be carried out to quantify the effects of coincident deformation on oxidation kinetics and mechanical properties of oxidized Zr-4 fuel cladding material.

3. Additional tests should be carried out to obtain more quantitative data for the linear reaction rate constants for both parent and braze HAZ materials.

4. Additional metallography of intermediately - severely oxidized samples should be performed to establish more precisely what microstructural features are characteristic of, or precursors to, loss of fracture toughness.

5. Additional oxidation tests should be carried out in a steam environment.

6. A few additional biaxial tests should be carried out at temperatures in the range 673-873 K to establish whether the transition zone can balloon preferentially at intermediate temperatures.

ACKNOWLEDGEMENTS

The authors wish to thank Mr. J.H.K. Lau of the Nuclear Studies and Safety Department of the Design and Development - Generation Division and Mr. J. Novak of the Fuel and Physics Department of the Technical and Training Services Division for useful discussions during the

course of the experimental work. We also wish to thank Mr. N. Graham of WCL, Port Hope, for supplying the fuel cladding material. Lastly, we wish to thank Mr. M.J. McGraw for carrying out the tensile testing.

Recommended by:

R.G. Fleck
Supervising Engineer
Materials Integrity Section

Prepared by:

E.T.C. Ho
Engineer - Metallurgical
Materials Integrity Section
Metallurgical Research Department

Approved by:

J. Brown
Manager
Metallurgical Research Department

A. Donner
Technologist
Materials Integrity Section
Metallurgical Research Department

ETCH/AD:ljh

REFERENCES

1. M. Wolicky, Ontario Hydro Research Division Report No. CS73-210-K, December 31, 1973.
2. F.W. Doyle, "Air Oxidation of Zircaloy-4 Sheathing", Central Nuclear Services Report No. CNS-IR-193, February, 1974.
3. E.T.C. Ho, Ontario Hydro Research Division Report No. M84-157-K, November 30, 1984.
4. E.T.C. Ho and A. Donner, Ontario Hydro Research Division Report No. 86-342-K, February 16, 1987.
5. N. Graham, Westinghouse Canada Limited, private communication.
6. D.O. Hobson and P.L. Rittenhouse, "Embrittlement of Zircaloy-Clad Fuel Rods by Steam during LOCA Transients", ORNL-4758, Oak Ridge National Laboratory, 1972.
7. R.E. Pawel, J. Nucl. Mater., 50, 247 (1974).
8. A. Sawatzky, "A Proposed Criterion for the Oxygen Embrittlement of Zircaloy-4 Fuel Cladding", Zirconium in the Nuclear Industry, ASTM STP 681, American Society for Testing and Materials, 479 (1979).
9. H.M. Chung, A.M. Garde and T.F. Kassner, "Development of an Oxygen Embrittlement Criterion for Zircaloy Cladding Applicable to Loss-of-Coolant Accident Conditions in Light-Water Reactors", Zirconium in the Nuclear Industry, ASTM STP 681, American Society for Testing and Materials, 600 (1979).
10. United States Atomic Energy Commission Docket No. RM-50-1, December, 1973.
11. D.O. Hobson, "Ductile-Brittle Behaviour of Zircaloy Fuel Cladding", Proceedings of the Topical Meeting of Water Reactor Safety, 26-28 March 1973, Salt Lake City, Utah.
12. E. Hillner, "The High-Temperature Oxidation Kinetics of Zirconium in Dry Oxygen", Electrochem. Technol. 4, 132 (1966).
13. V. Urbanic, J. Electrochem. Soc., 119, 1527 (1972).
14. R. Kohli, J. Nucl. Mater., 91, 85 (1980).
15. M. Suzuki and S. Kawasaki, J. Nucl. Mater., 140, 32 (1986).
16. S. Leistikow, G. Schanz, H.V. Berg and A.E. Aly, "Comprehensive Presentation of Extended Zircaloy-4 Steam Oxidation Results 600-1600°C", Conference Proceedings, Risø National Laboratory, May 16-20, 1983.

17. J.H.K. Lau, Memorandum to C. Lee, "Time-to-Fuel-Failure Assessment", File: 906-NA44-03500 T5, October 7, 1983.

18. S. Sagat, Memorandum to H.E. Sills, "Low Temperature Sheath Oxidation", AECL-CRNL, Fuel Engineering Branch, July 17, 1984.

TABLE I

SUMMARY OF OXIDATION TEST RESULTS

SPECIMEN		PARENT MATERIAL		BRAZE HAZ MATERIAL	
TEMP (K)	TIME	OXIDE (mm)	METAL (mm)	OXIDE (mm)	METAL (mm)
873 *	3 days	0.045	0.360	0.085	0.320
873 *	6 days	0.100	0.270	0.190	0.190
873	6 days	0.105	0.340	0.180	0.305
873	9 days	0.130	0.330	0.280	0.265
873 *	9 days	0.165	0.183	0.304	0.049
873	15 days	0.260	0.252	0.450	0.152
923 *	1 day	0.047	0.338	0.071	0.326
923	2 days	0.070	0.364	0.160	0.317
923	3 days	0.152	0.310	0.280	0.246
923	4 days	0.171	0.304	0.328	0.227
923	5 days	0.260	0.236	0.508	0.115
923	5 days	0.243	0.242	0.494	0.109
973	6 hrs	0.038	0.411	0.070	0.396
973	6 hrs	0.027	0.394	0.052	0.385
973	24 hrs	0.108	0.348	0.226	0.292
973	24 hrs	0.133	0.322	0.210	0.284
973	48 hrs	0.313	0.221	0.512	0.112
1023	3 hrs	0.0095	0.411	0.051	0.378
1023	6 hrs	0.063	0.362	0.115	0.347
1023	18 hrs	0.247	0.248	0.370	0.192
1073	2 hrs	0.0081	0.413	0.061	0.380
1073	4 hrs	0.091	0.351	0.156	0.332
1073	8 hrs	0.221	0.268	0.343	0.202
1123	1 hr	0.010	0.415	0.043	0.392
1123	2 hrs	0.088	0.318	0.126	0.351
1123	4 hrs	0.232	0.185	0.314	0.224

* double-sided or ID/OD oxidation

TABLE II

SUMMARY OF TENSILE TEST RESULTS

SPECIMEN		PARENT MATERIAL			BRAZE HAZ MATERIAL		
TEMP (K)	TIME	YS* (MPa)	PS# (MPa)	AEF+ ($\times 10^5$ J/m^2)	YS (MPa)	PS (MPa)	AEF ($\times 10^5$ J/m^2)
873	6 days	488±12	600.6±6.8	6.06±1.09	479	596	3.61
873	9 days	512±13	640.9±10.3	2.12±0.48	478	579	1.12
873	15 days	559±15	625.0±26.7	1.04±0.07	--	--	0.32
923	2 days	468±9	560.3±4.8	7.41±0.37	510	626	4.89
923	3 days	441±8	585.5±13.5	6.92±1.13	441	596	2.92
923	4 days	483±4	626.8±26.5	4.63±0.47	513	656	2.52
923	5 days	476±30	626.8±7.8	3.78±0.92	619	655	1.81
973	6 hrs	441±6	544.4±2.3	9.05±1.47	433	582	5.20
973	24 hrs	441±5	553.7±4.1	7.19±0.93	480	617	5.17
973	48 hrs	520±51	683.8±12.9	3.62±0.72	--	--	0.93
1023	3 hrs	461±8	577.3±3.5	5.81±0.36	475	620	5.98
1023	6 hrs	480±10	615.0±9.3	7.55±0.88	459	618	4.90
1023	18 hrs	514±15	644.8±16.1	4.13±0.31	460	537	1.81
1073	2 hrs	449±3	581.3±4.8	5.43±0.50	445	597	4.84
1073	4 hrs	480±16	616.3±23.8	5.06±0.70	471	618	4.98
1073	8 hrs	497±24	602.9±59.2	3.04±0.43	506	656	2.20
1123	1 hr	447±9	554.6±5.6	4.10±0.38	454	597	4.72
1123	2 hrs	512±21	605.1±36.3	3.22±0.99	475	618	3.04
AS-RECEIVED		531±15	594.3±13.1	10.47±1.75	403.7 ±16.9	536.7 ±11.2	6.42 ±1.11

* YS - estimated yield strength
\# PS - peak or maximum engineering stress (equivalent to UTS in most cases)
\+ AEF- estimated energy absorbed to fracture

TABLE III

SUMMARY OF FRACTURE ENERGY RESULTS

SPECIMEN		PARENT MATERIAL		BRAZE HAZ MATERIAL	
TEMP (K)	TIME	% WALL OXIDIZED	AEF* ($\times 10^5$ J/m^2)	% WALL OXIDIZED	AEF ($\times 10^5$ J/m^2)
873	6 days	18.9	6.06±1.09	27.2	3.61
873	9 days	21.2	2.12±0.48	36.8	1.12
873	15 days	39.9	1.04±0.07	63.7	0.32
923	2 days	13.1	7.41±0.37	24.3	4.89
923	3 days	26.0	6.92±1.13	41.3	2.92
923	4 days	27.5	4.62±0.47	45.8	2.52
923	5 days	43.7	3.78±0.92	72.6	1.81
973	6 hrs	1.9	9.05±1.47	5.5	5.20
973	24 hrs	16.9	7.19±0.93	30.3	5.17
973	48 hrs	47.3	3.62±0.72	73.3	0.93
1023	3 hrs	1.9	5.81±0.36	9.8	5.98
1023	6 hrs	13.6	7.55±0.88	17.2	4.90
1023	18 hrs	40.8	4.13±0.31	54.2	1.81
1073	2 hrs	1.4	5.43±0.50	9.3	4.84
1073	4 hrs	16.2	5.06±0.70	20.8	4.98
1073	8 hrs	36.0	3.04±0.43	51.8	2.20
1123	1 hr	0.95	4.10±0.38	6.4	4.72
1123	2 hrs	24.1	3.22±0.99	16.2	3.04
AS-RECEIVED		--	10.47±1.75	--	6.42±1.11

* AEF - estimated energy absorbed to fracture.

TABLE IV

SUMMARY OF LEAST SQUARES PARAMETER VALUES *

TEST CONDITION		INTERCEPT (a) (mm)	SLOPE (b) (mm/h)
MATERIAL TYPE	TEMP (K)		
Parent	873	-0.00679	0.000734
Braze HAZ	873	0.00350	0.00127
Parent	923	-0.0175	0.00218
Braze HAZ	923	-0.0473	0.00443
Parent	973	-0.0177	0.00655
Braze HAZ	973	-0.0148	0.0106
Parent	1023	-0.0347	0.0157
Braze HAZ	1023	-0.0127	0.0213
Parent	1073	-0.0569	0.0351
Braze HAZ	1073	-0.0325	0.0470
Parent	1123	-0.0620	0.0737
Braze HAZ	1123	-0.0510	0.0909

* $\delta = a + bt$, where δ is in millimeters and t is in hours

TABLE V

SUMMARY OF PSEUDO-LINEAR REACTION RATE CONSTANTS

OXIDATION TEMP (K)	PARENT MATERIAL k_L (cm/s)	BRAZE HAZ MATERIAL k_L (cm/s)
873	2.039×10^{-8}	3.528×10^{-8}
923	6.056×10^{-8}	1.231×10^{-7}
973	1.819×10^{-7}	2.944×10^{-7}
1023	4.361×10^{-7}	5.917×10^{-7}
1073	9.750×10^{-7}	1.306×10^{-6}
1123	2.047×10^{-6}	2.525×10^{-6}

TABLE VI

COMPARISONS OF OXIDATION RATE CORRELATIONS WITH LITERATURE DATA

OXIDATION CONDITION	OXIDE THICKNESS (mm) OHRD PARENT MATERIAL CORRELATION PREDICTION	OXIDE THICKNESS (mm) LITERATURE DATA (REFERENCE)
873 K - 25 h	0.0116	0.0146 (1)
923 K - 25 h	0.0175	0.0370 (1)
973 K - 25 h	0.1461	0.0695 (1)
1023 K - 25 h	0.3578	0.2239 (1)
1073 K - 25 h	0.8206	0.2801 (1)
1123 K - 25 h	1.7805	0.0340 (1)
1023 K - 14 h	0.1851	0.190 (2)
1023 K - 20 h	0.2793	0.290 (2)
1123 K - 2.1 h	0.0928	0.017-0.120 (2)

(1) Leistikow et al (reference 13)
(2) Sagat (reference 15)

(a)

(b)

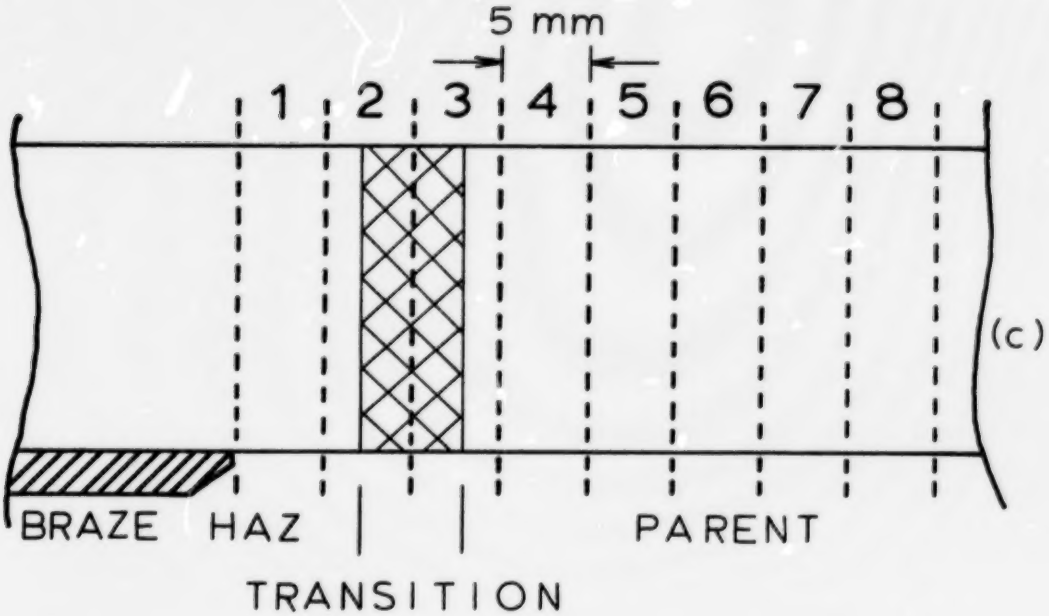

FIGURE 1: PHOTOGRAPHS OF OXIDIZED SAMPLES AND A SCHEMATIC DIAGRAM ILLUSTRATING THE LOCATIONS OF RING SAMPLES REMOVED FOR TENSILE TESTING.

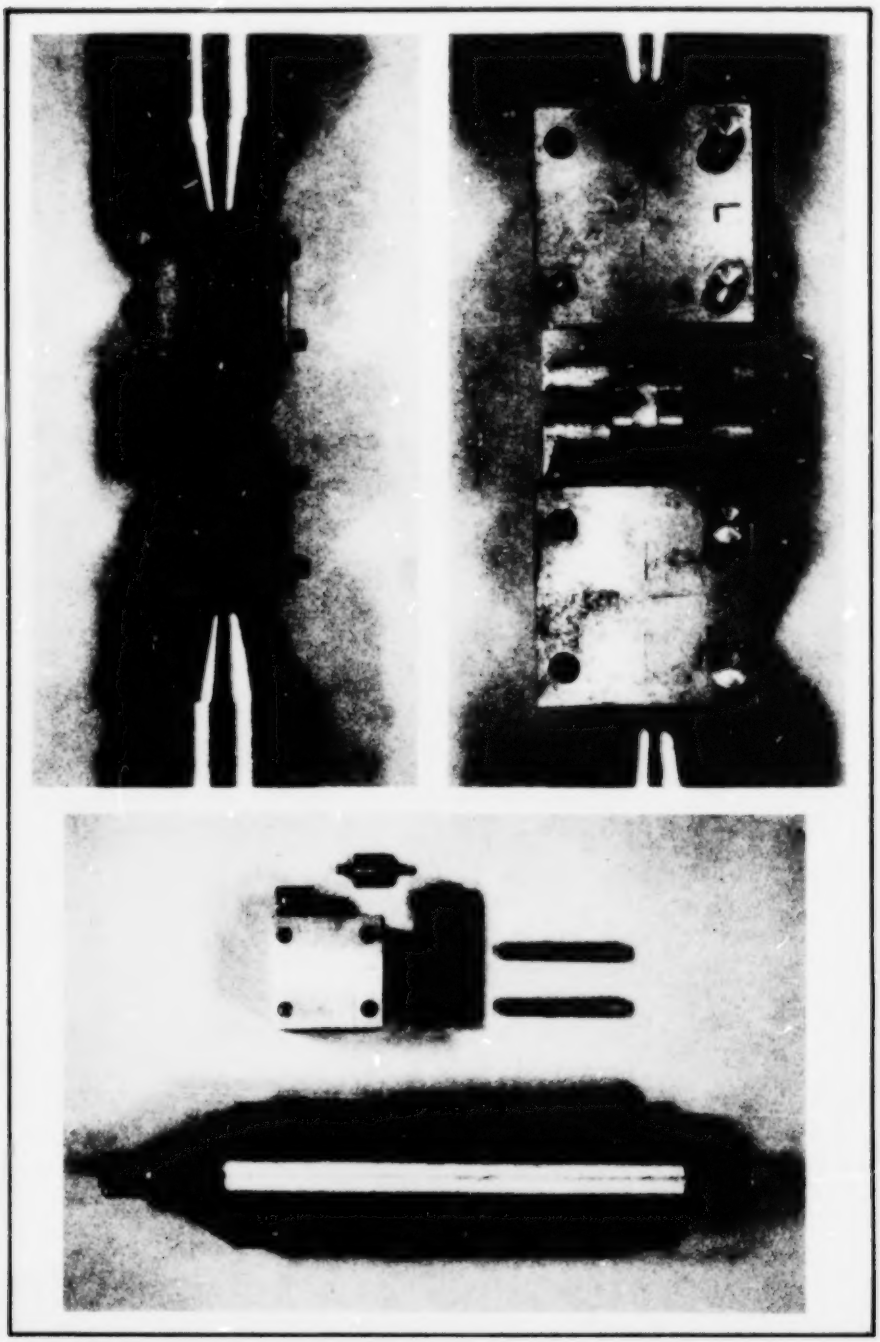

FIGURE 2: PHOTOGRAPHS ILLUSTRATING THE COMPONENTS OF THE FIXTURE DESIGNED FOR CARRYING OUT TENSILE TESTING OF RING FUEL CLADDING SAMPLES.

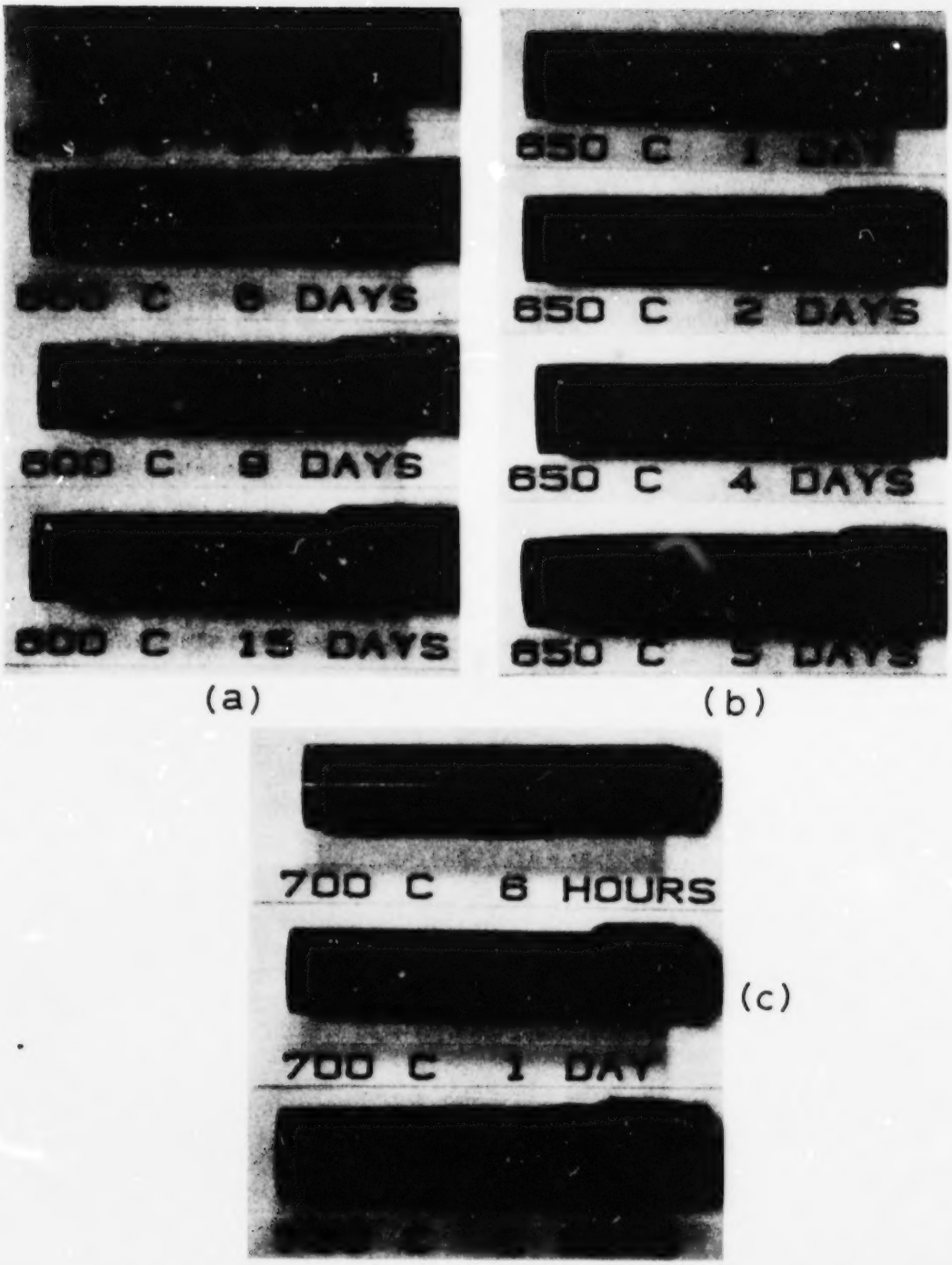

FIGURE 3: PHOTOGRAPHS ILLUSTRATING THE APPEARANCE OF ONE HALF OF THE CENTRAL MONITORED ZONE OF SPECIMENS OXIDIZED FOR VARIOUS TIMES AT: (a) 873 K; (b) 923 K; (c) 973 K.

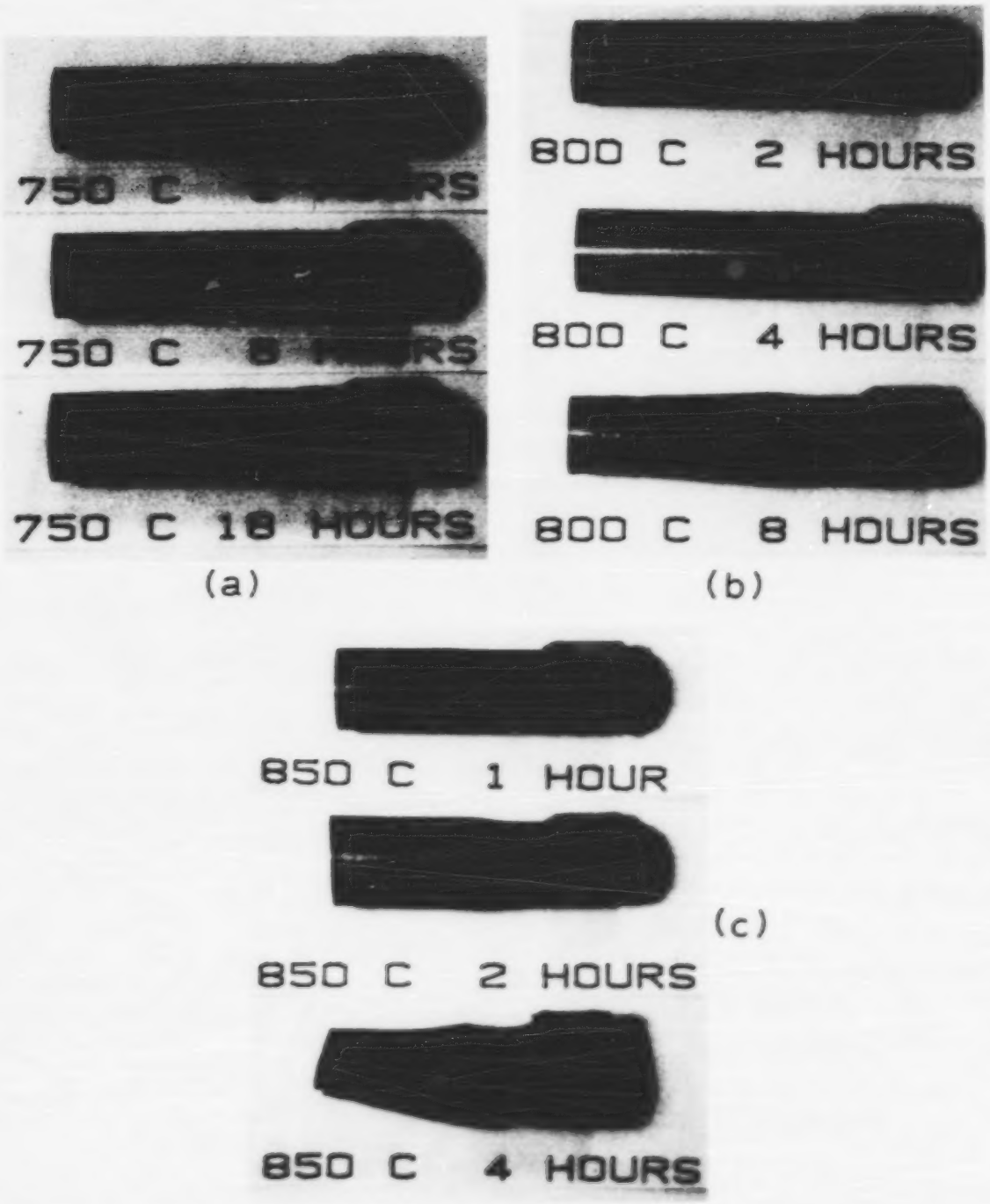

FIGURE 4: PHOTOGRAPHS ILLUSTRATING THE APPEARANCE OF ONE HALF OF THE CENTRAL MONITORED ZONE OF SPECIMENS OXIDIZED FOR VARIOUS TIMES AT: (a) 1023 K; (b) 1073 K; (c) 1123 K.

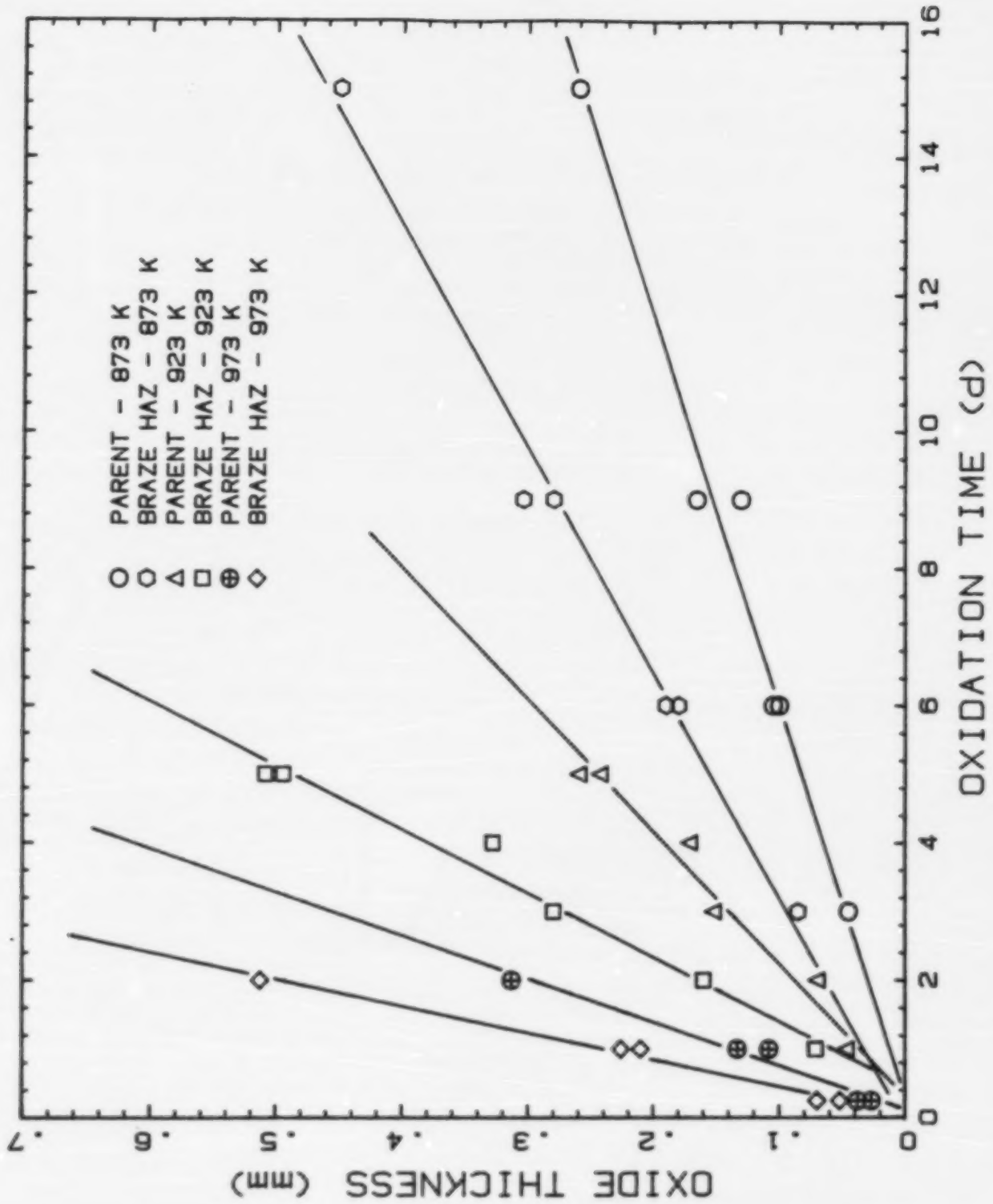

FIGURE 5: PLOTS ILLUSTRATING THE POST-TRANSITION OXIDATION KINETIC BEHAVIOUR OF PARENT AND BRAZE HAZ MATERIALS AT 873, 923 AND 973 K.

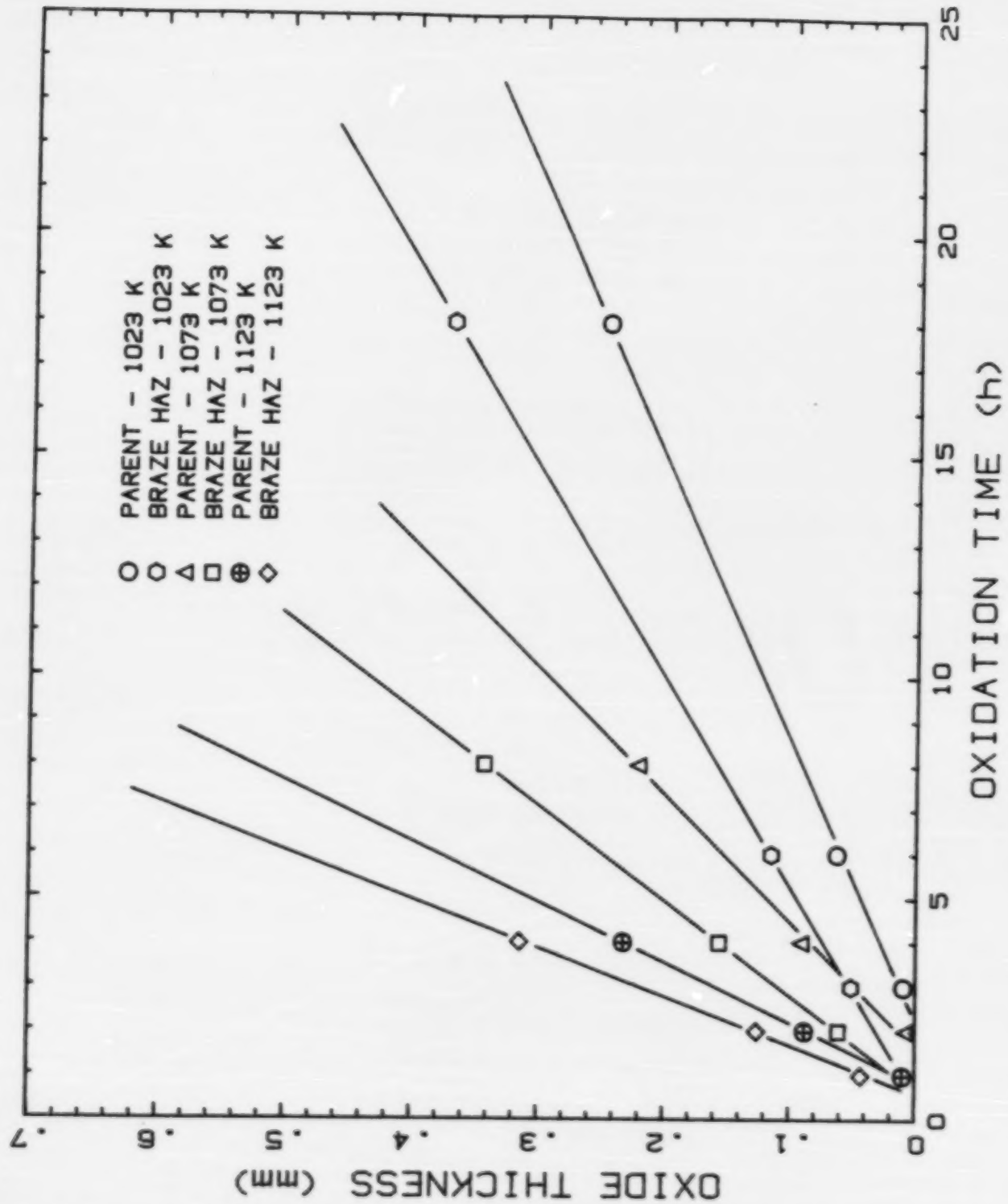

FIGURE 6: PLOTS ILLUSTRATING THE POST-TRANSITION OXIDATION KINETIC BEHAVIOUR OF PARENT AND BRAZE HAZ MATERIALS AT 1023, 1073 AND 1123 K.

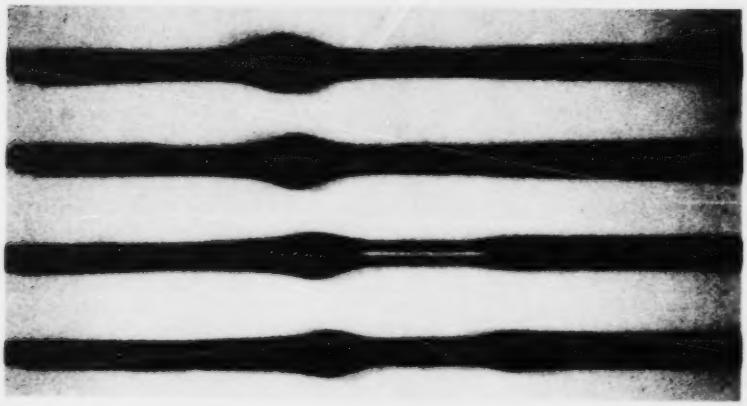

FIGURE 7: PHOTOGRAPH ILLUSTRATING THE APPEARANCE OF SAMPLES DEFORMED AT ELEVATED TEMPERATURES UNDER RELATIVELY HIGH INTERNAL PRESSURES.

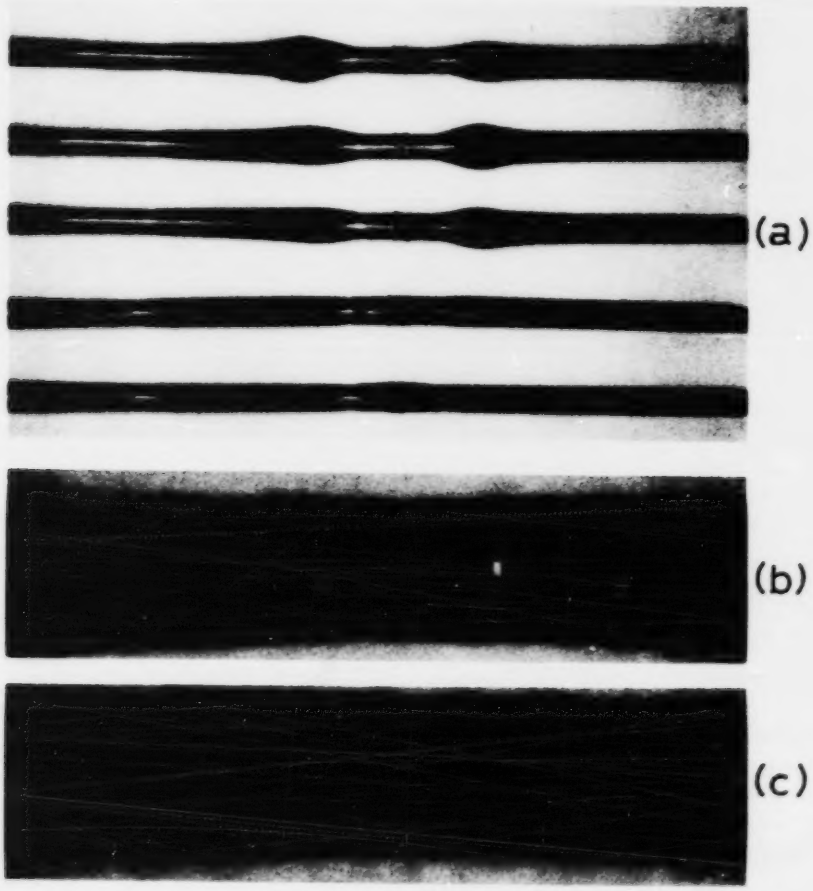

FIGURE 8: PHOTOGRAPHS ILLUSTRATING THE APPEARANCE OF TEST SAMPLES DEFORMED AT 973 K UNDER VARIOUS INTERNAL PRESSURES (a), AND THE LOCATION AND NATURE OF HAIRLINE CRACKS IN BRAZE HAZ MATERIAL AT LOW INTERNAL PRESSURES (b&c).

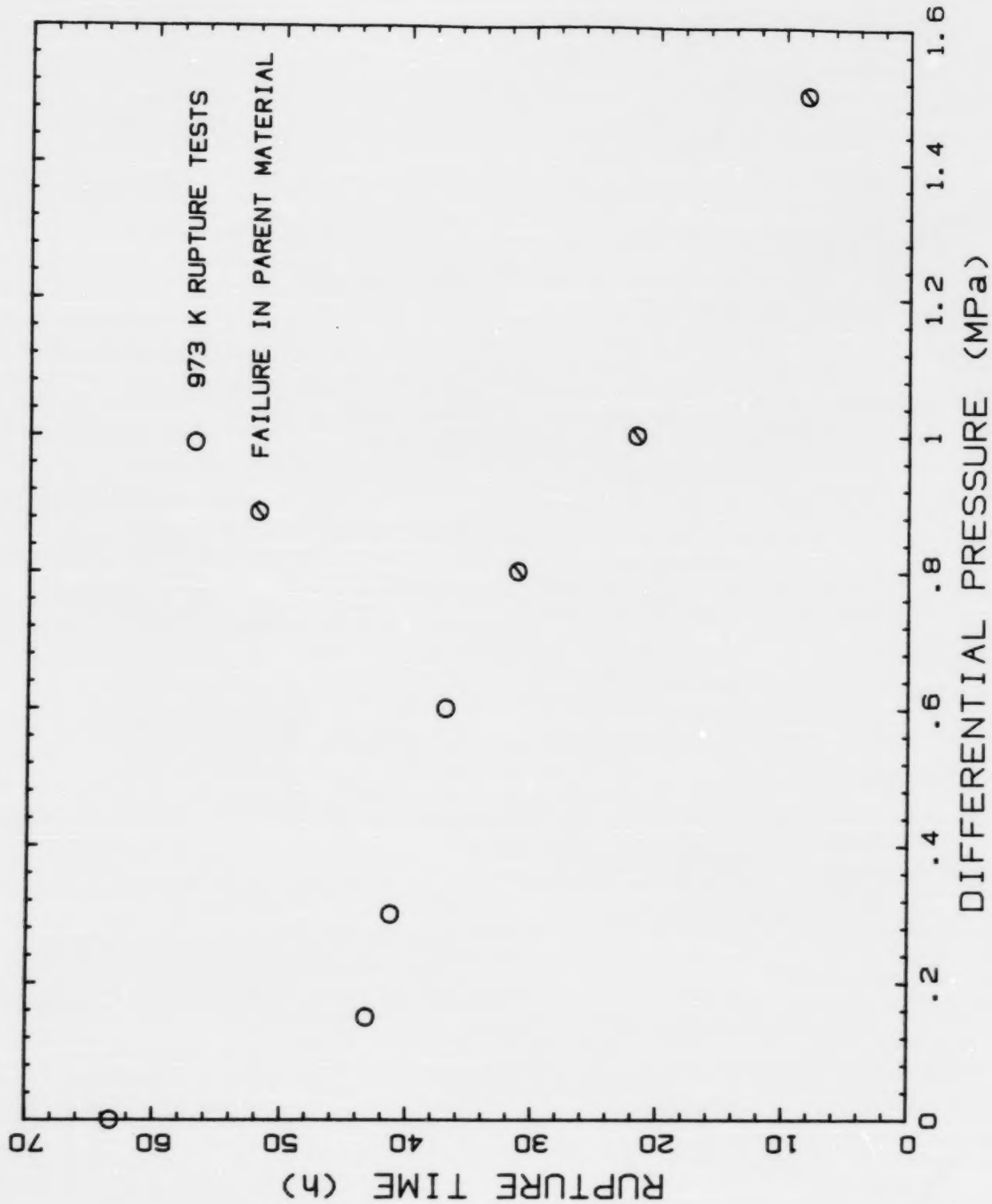

FIGURE 9. PLOT ILLUSTRATING THE VARIATION OF TIME TO FAILURE AS A FUNCTION OF INTERNAL PRESSURE AT 973 K.

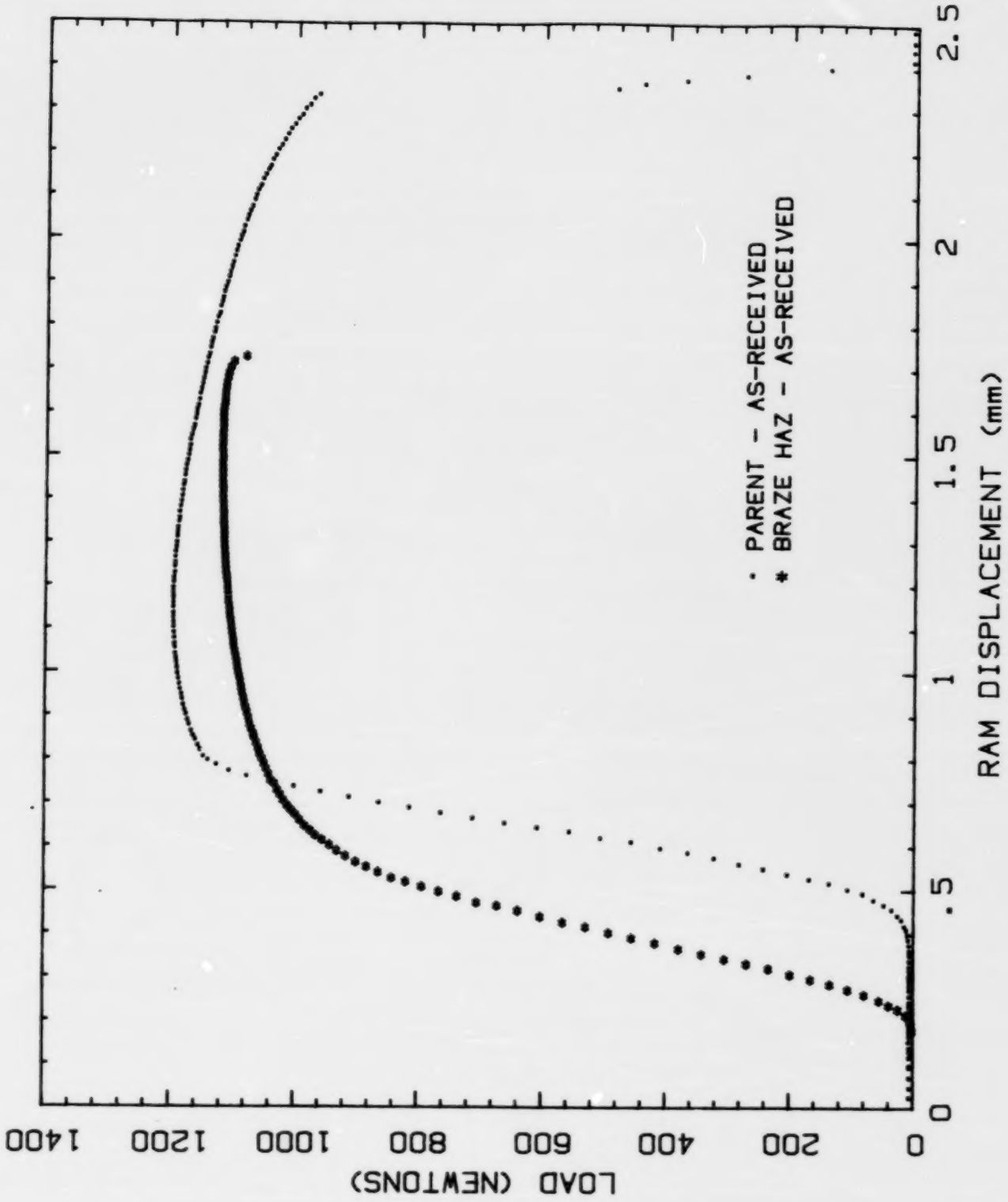

FIGURE 10: LOAD VS RAM DISPLACEMENT PLOTS FOR AS-RECEIVED PARENT AND BRAZE HAZ FUEL CLADDING MATERIALS.

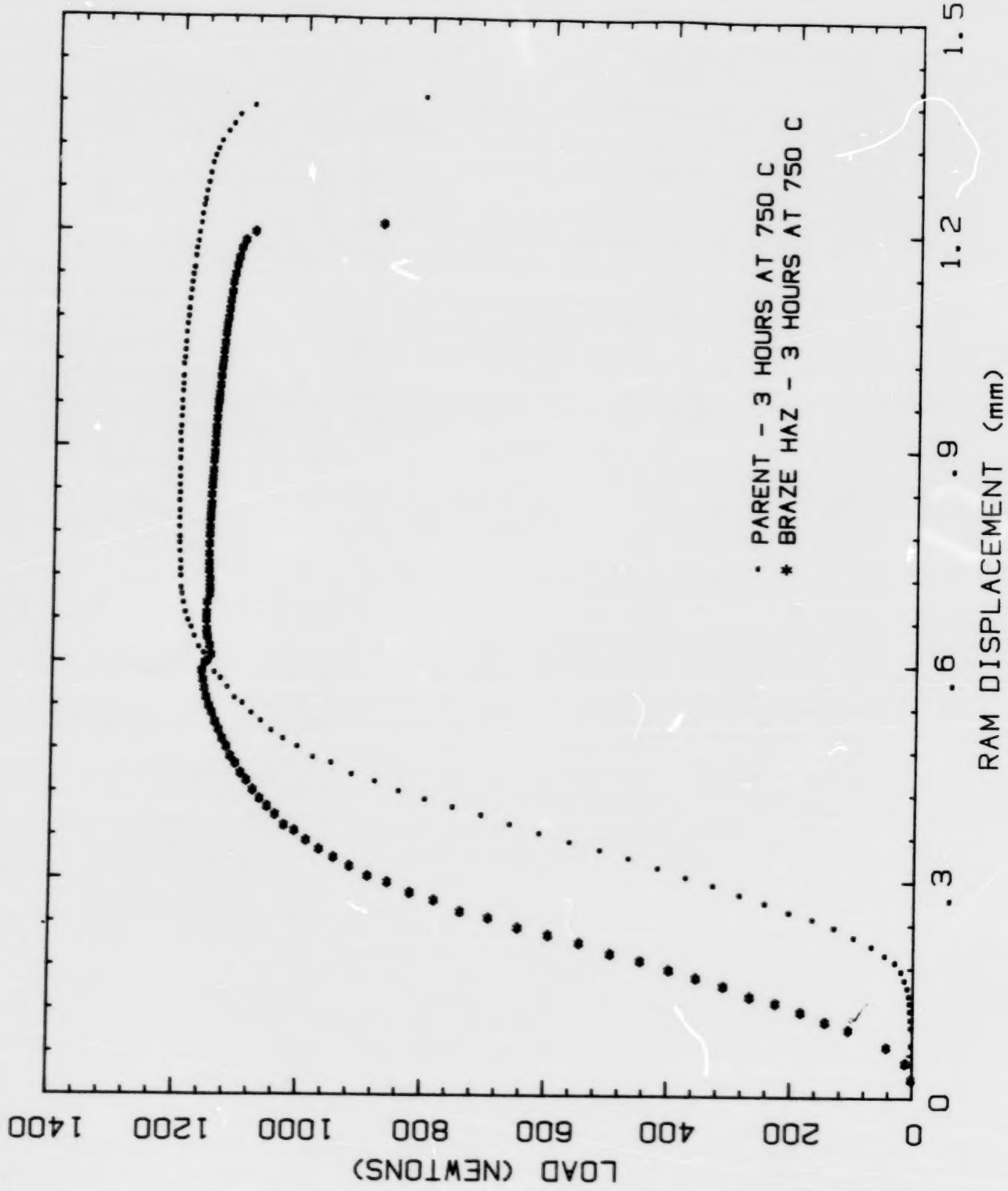

FIGURE 11: LOAD VS RAM DISPLACEMENT PLOTS FOR MILDLY OXIDIZED PARENT AND BRAZE HAZ FUEL CLADDING MATERIALS.

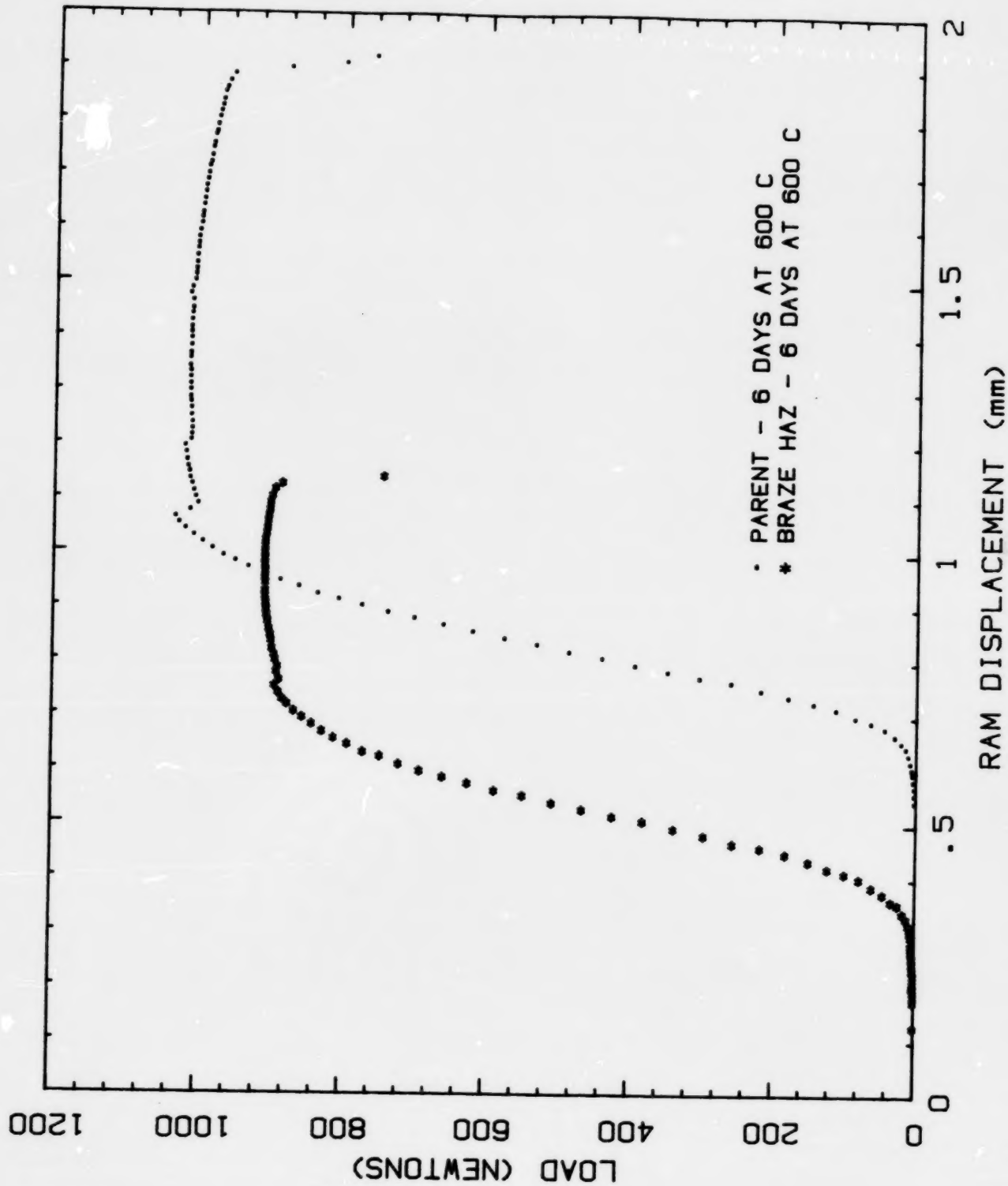

FIGURE 12: LOAD VS RAM DISPLACEMENT PLOTS FOR INTERMEDIATELY OXIDIZED PARENT AND BRAZE HAZ FUEL CLADDING MATERIALS.

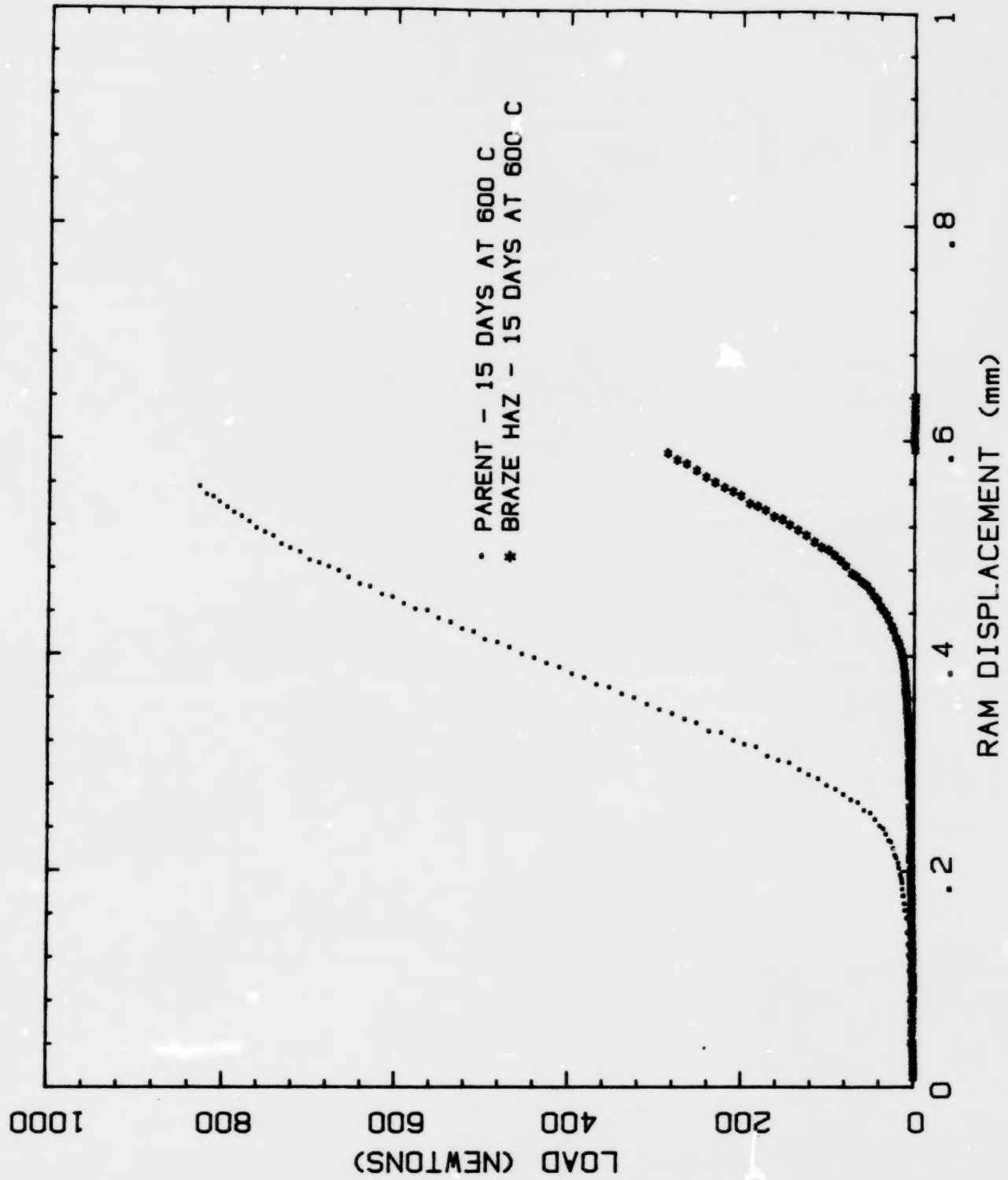

FIGURE 13: LOAD VS RAM DISPLACEMENT PLOTS FOR SEVERELY OXIDIZED AND EMBRITTLED PARENT AND BRAZE HAZ FUEL CLADDING MATERIALS.

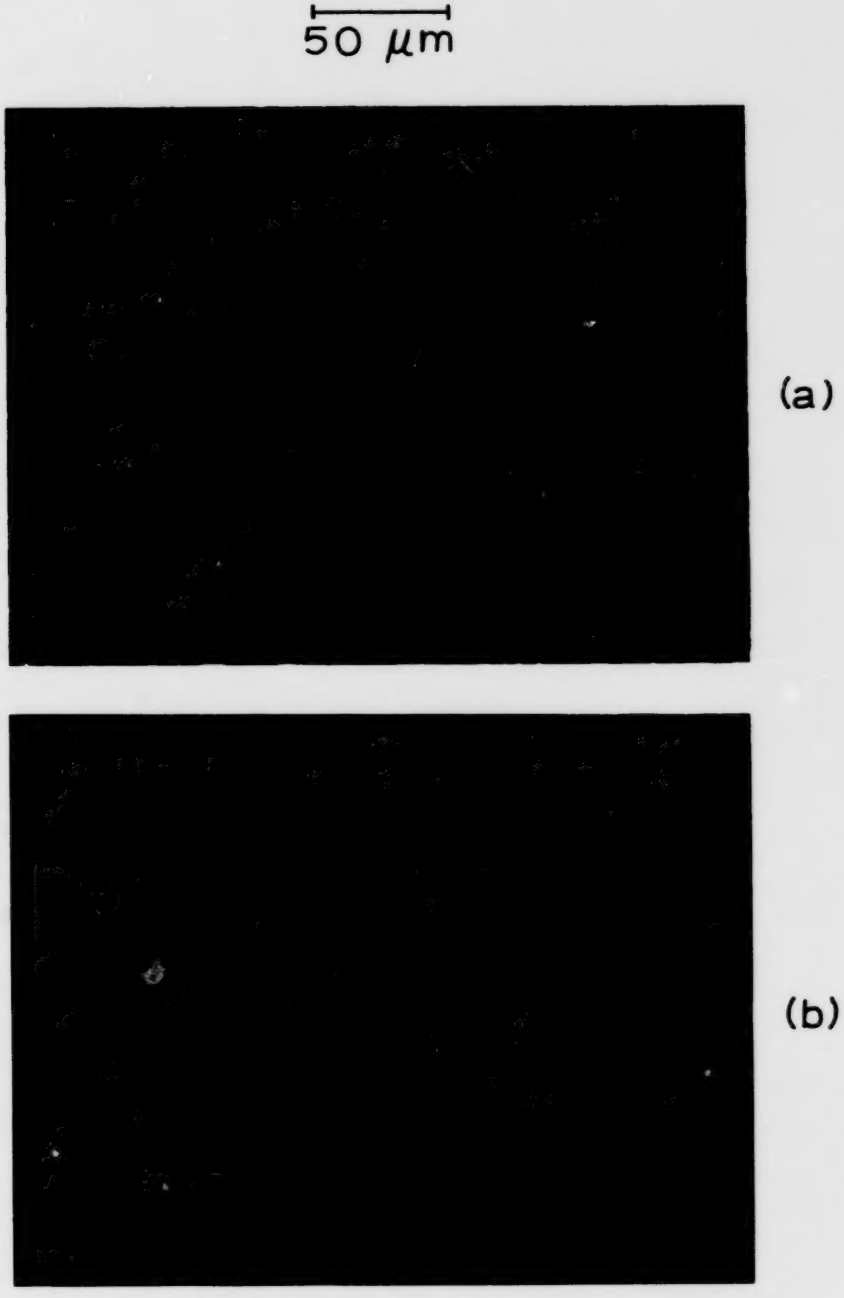

FIGURE 14: MICROGRAPHS ILLUSTRATING THE MICROSTRUCTURE OF AS-RECEIVED PARENT (a) AND BRAZE HAZ (b) FUEL CLADDING MATERIALS.

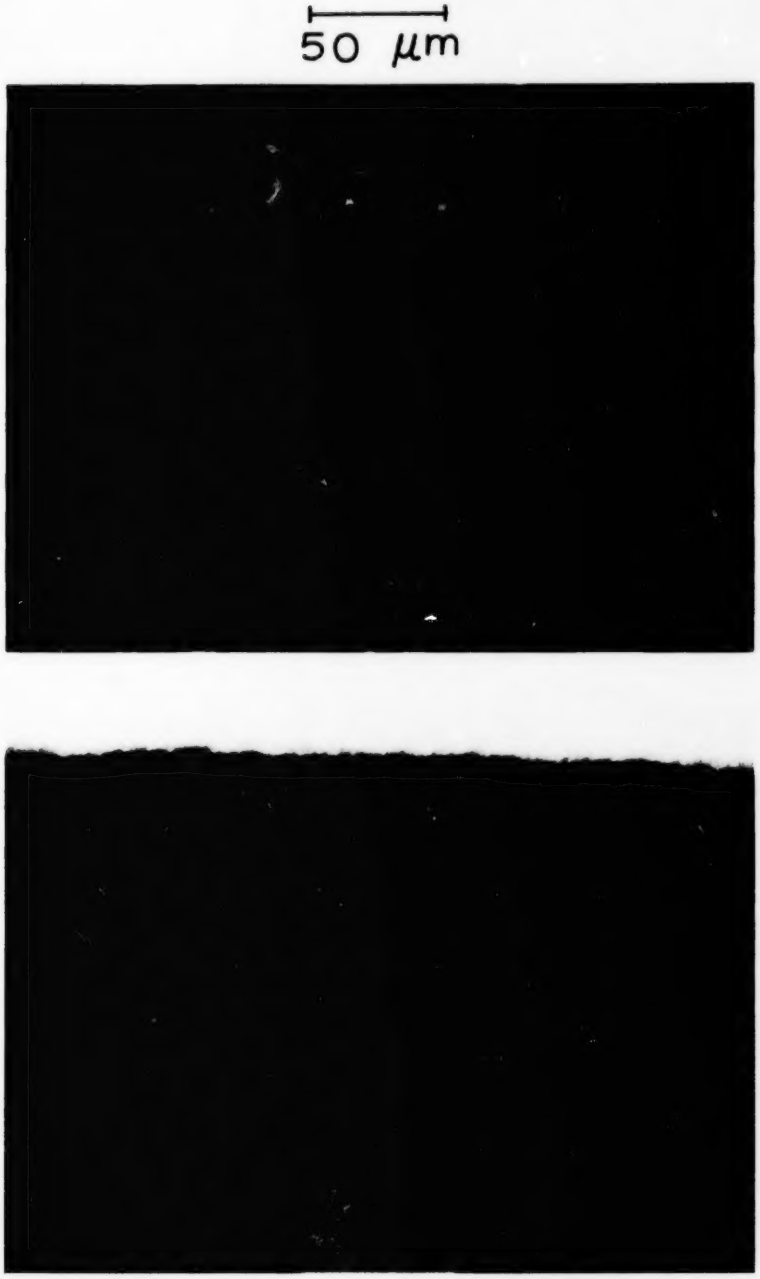

FIGURE 15. MICROGRAPHS ILLUSTRATING THE MICROSTRUCTURE OF OF MILDLY OXIDIZED (3 HOURS AT 1023 K) PARENT (a) AND BRAZE HAZ (b) FUEL CLADDING MATERIALS.

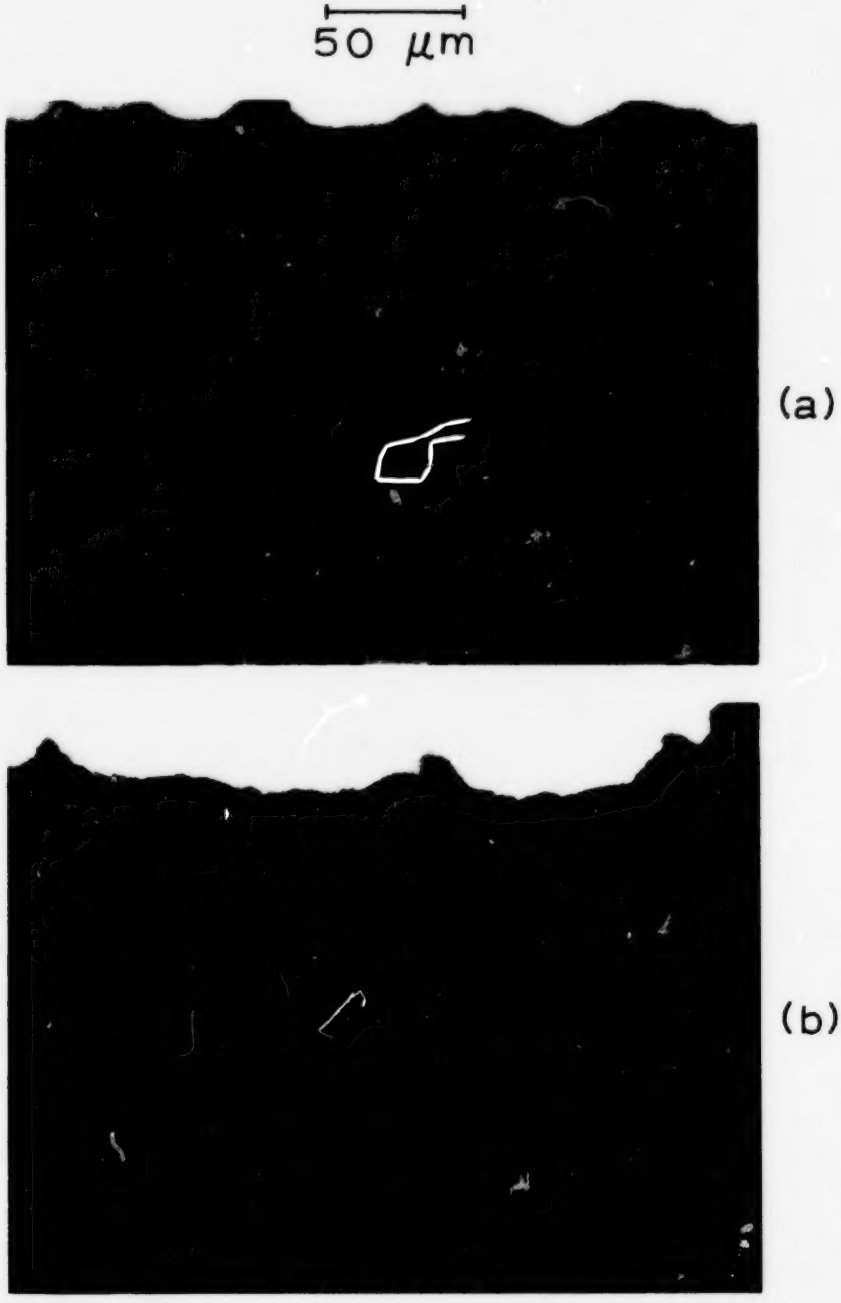

FIGURE 16: MICROGRAPHS ILLUSTRATING THE MICROSTRUCTURE OF INTERMEDIATELY OXIDIZED (6 DAYS AT 873 K) PARENT (a) AND BRAZE HAZ (b) FUEL CLADDING MATERIALS.

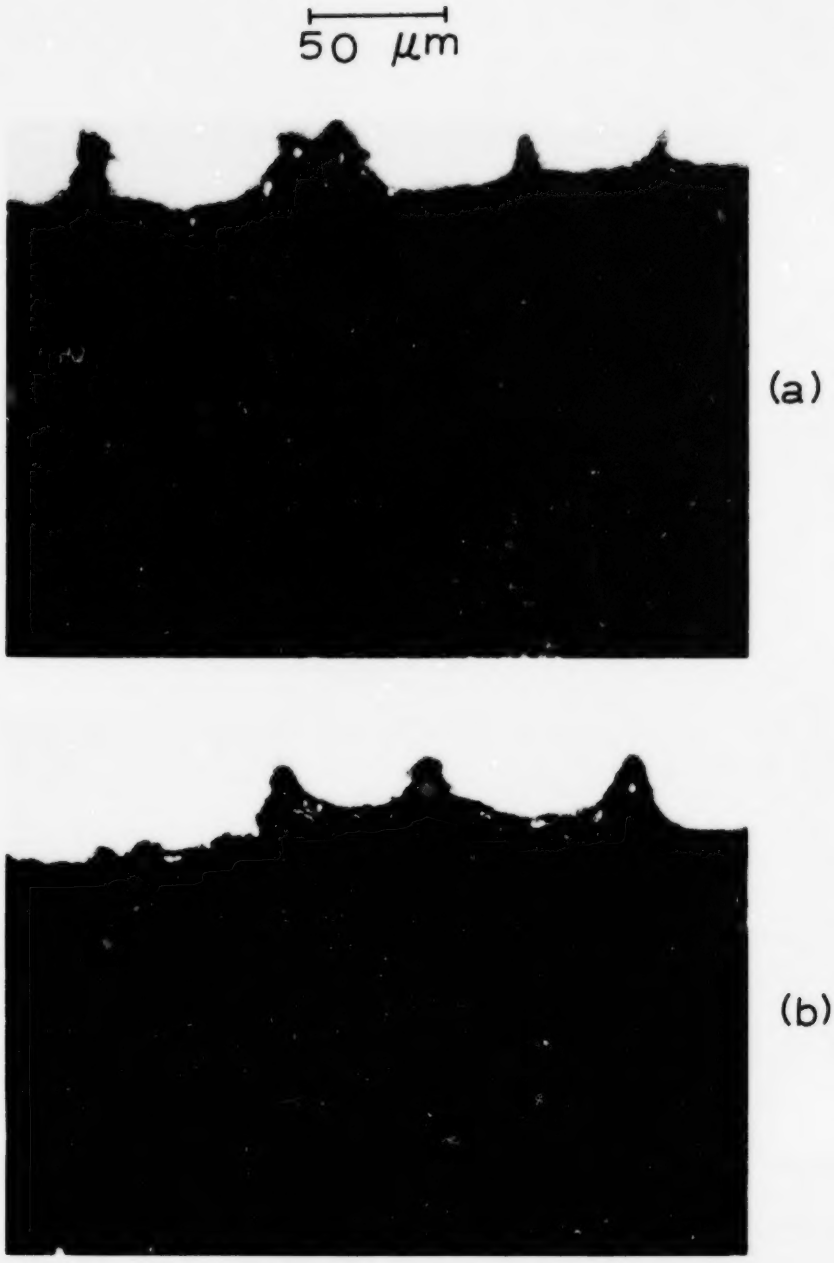

FIGURE 17: MICROGRAPHS ILLUSTRATING THE MICROSTRUCTURE OF SEVERELY OXIDIZED (15 DAYS AT 873 K) PARENT (a) AND BRAZE HAZ (b) FUEL CLADDING MATERIALS.

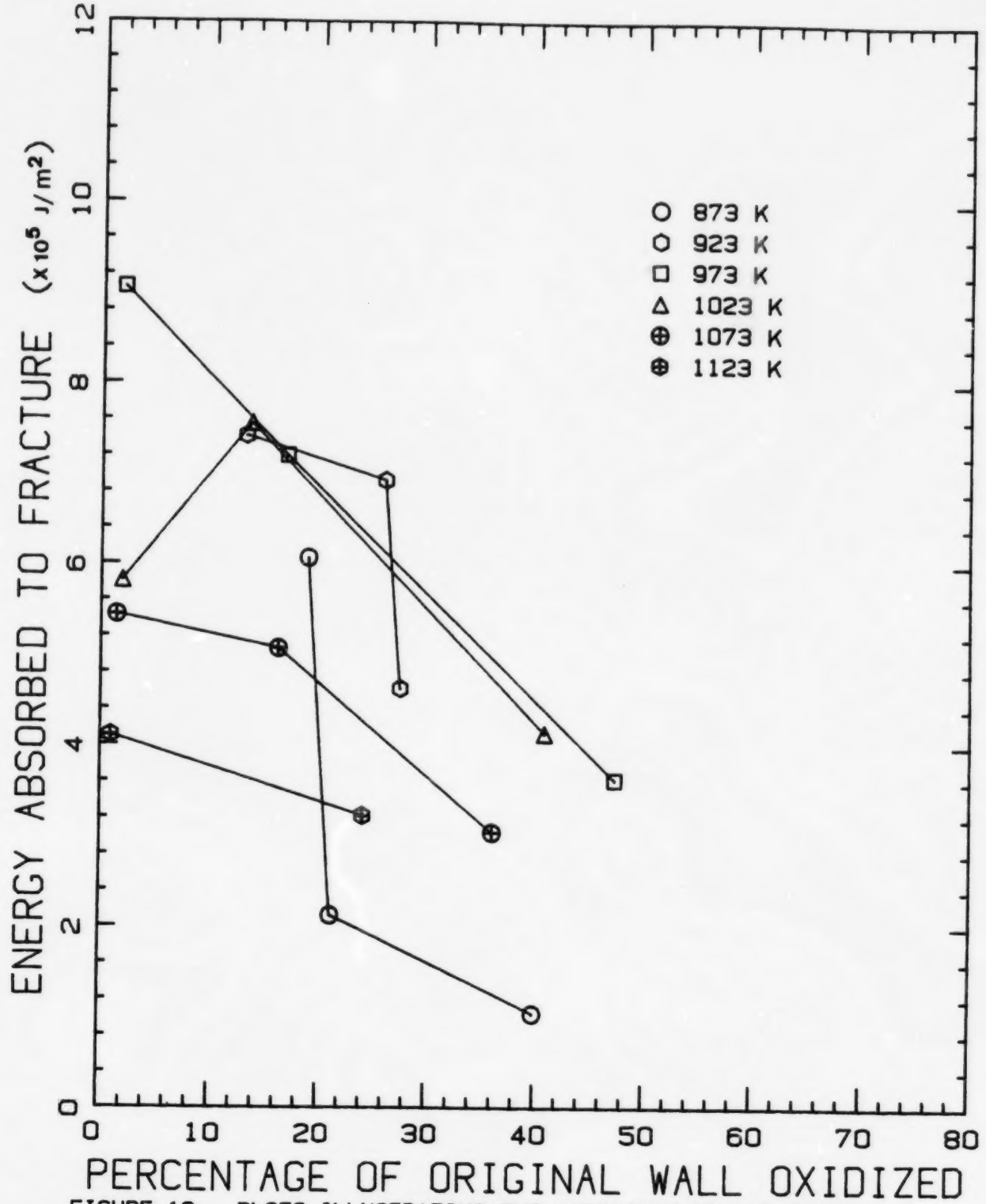

FIGURE 18: PLOTS ILLUSTRATING THE VARIATION OF THE ENERGY ABSORBED TO FRACTURE AT ROOM TEMPERATURE FOR PARENT CLADDING MATERIAL OXIDIZED AT 873, 923, 973, 1023, 1073 AND 1123 K.

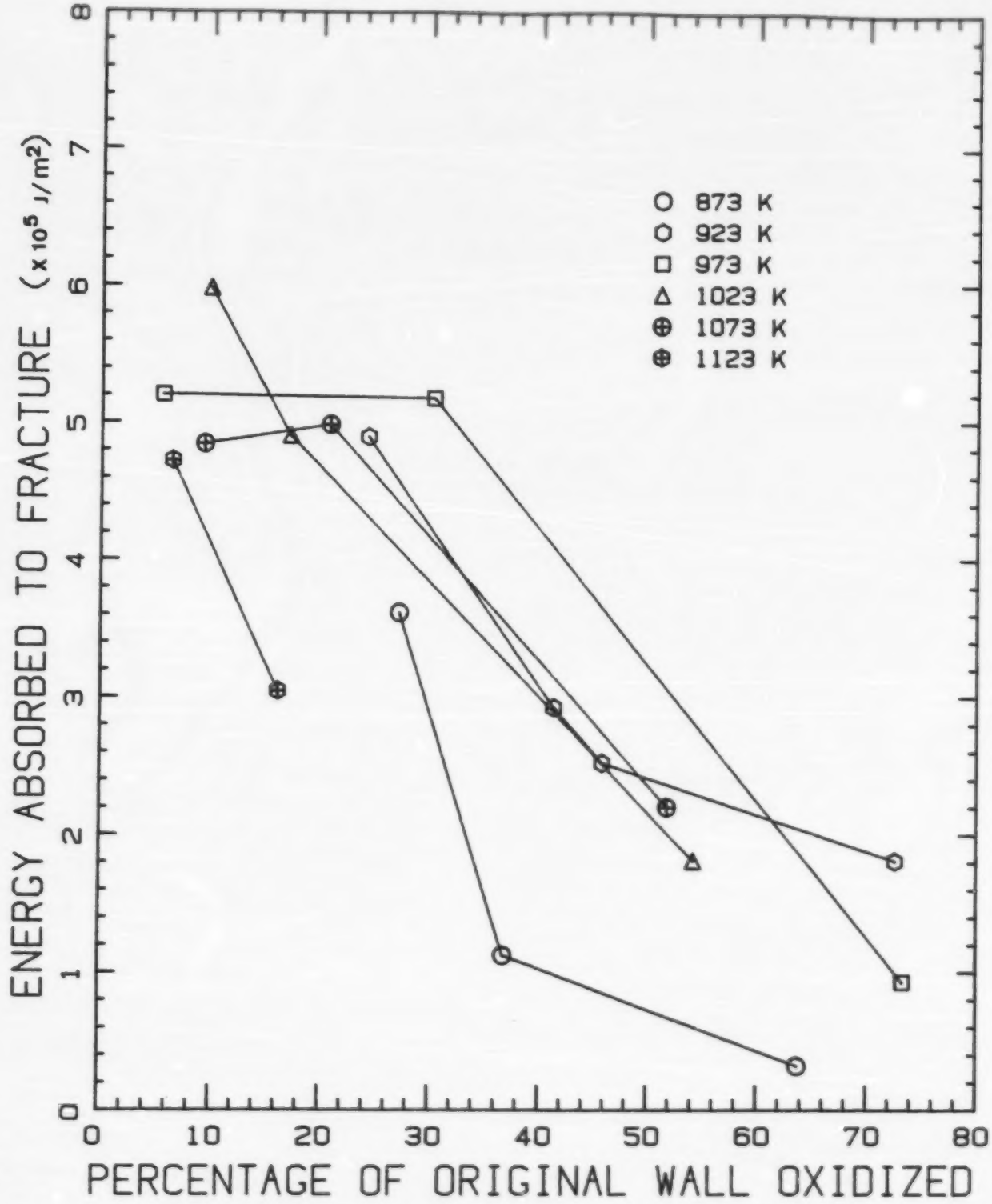

FIGURE 19. PLOTS ILLUSTRATING THE VARIATION OF THE ENERGY ABORBED TO FRACTURE AT ROOM TEMPERATURE FOR BRAZE HAZ CLADDING MATERIAL OXIDIZED AT 873, 923, 973, 1023, 1073 AND 1123 K.

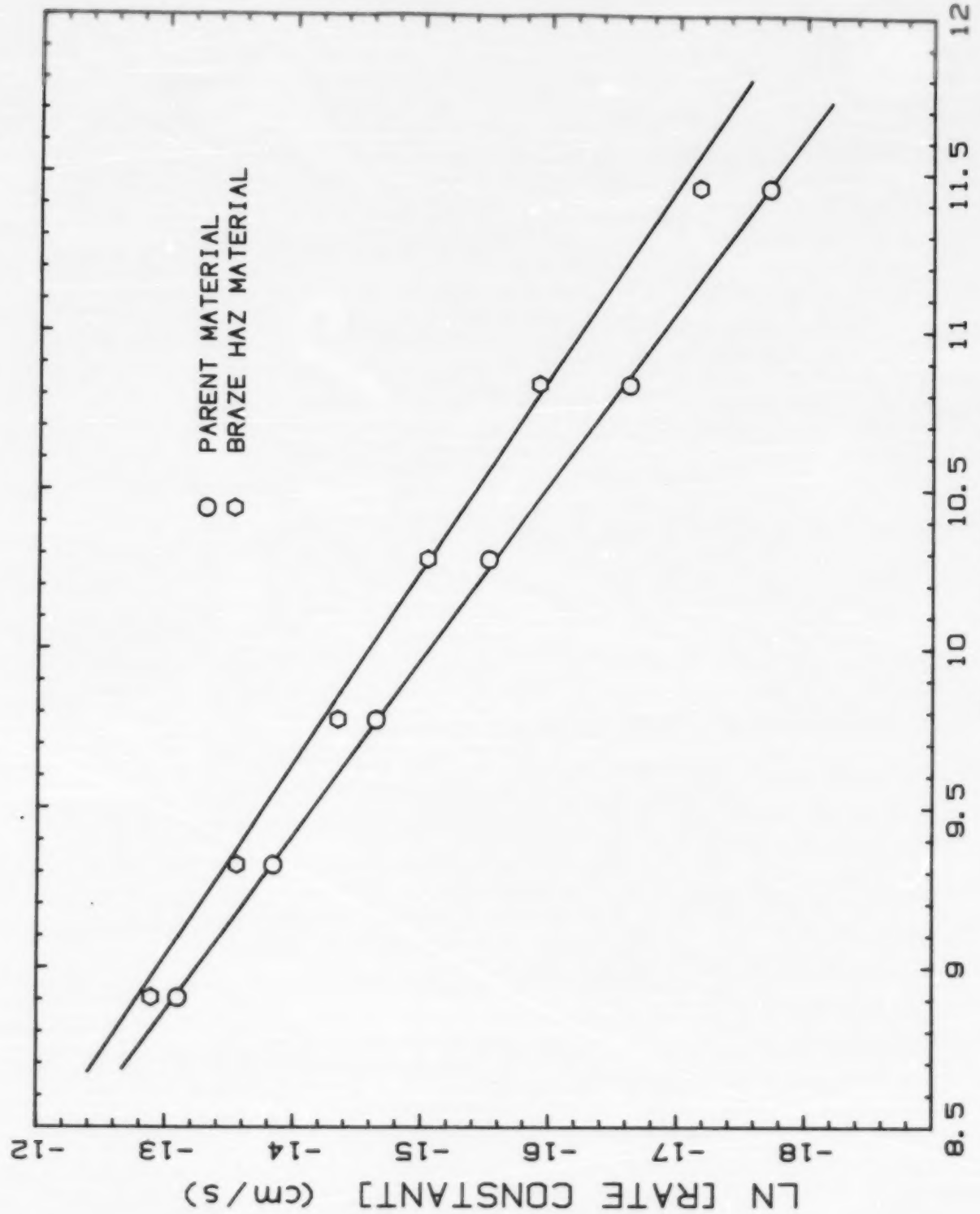

FIGURE 20: PLOTS ILLUSTRATING THE VARIATION OF PSEUDO-LINEAR REACTION RATE CONSTANTS WITH TEMPERATURE.

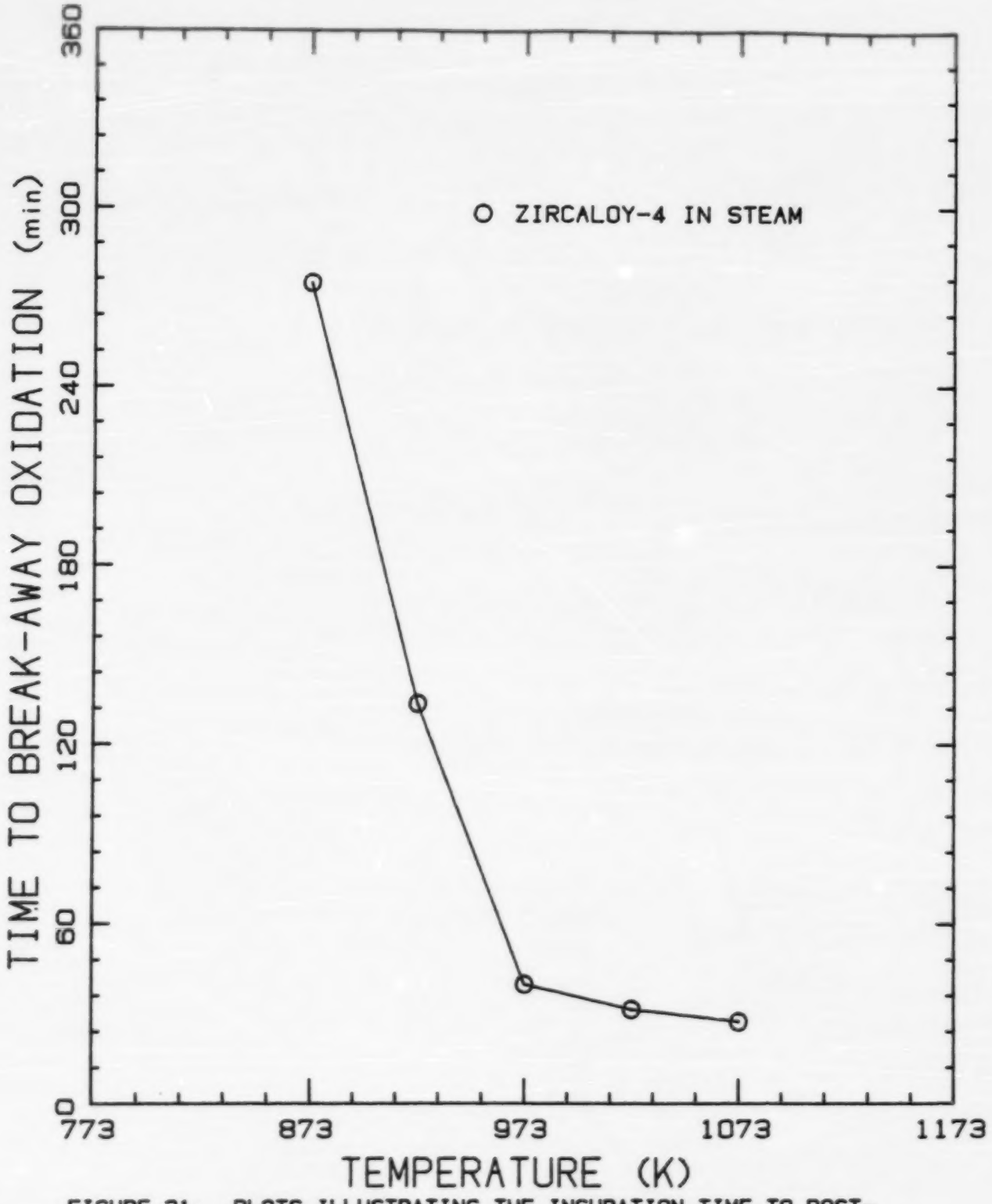

FIGURE 21: PLOTS ILLUSTRATING THE INCUBATION TIME TO POST-TRANSITION OR LINEAR OXIDATION BEHAVIOUR AS A FUNCTION OF TEMPERATURE FOR ZR-4 FUEL CLADDING MATERIAL.

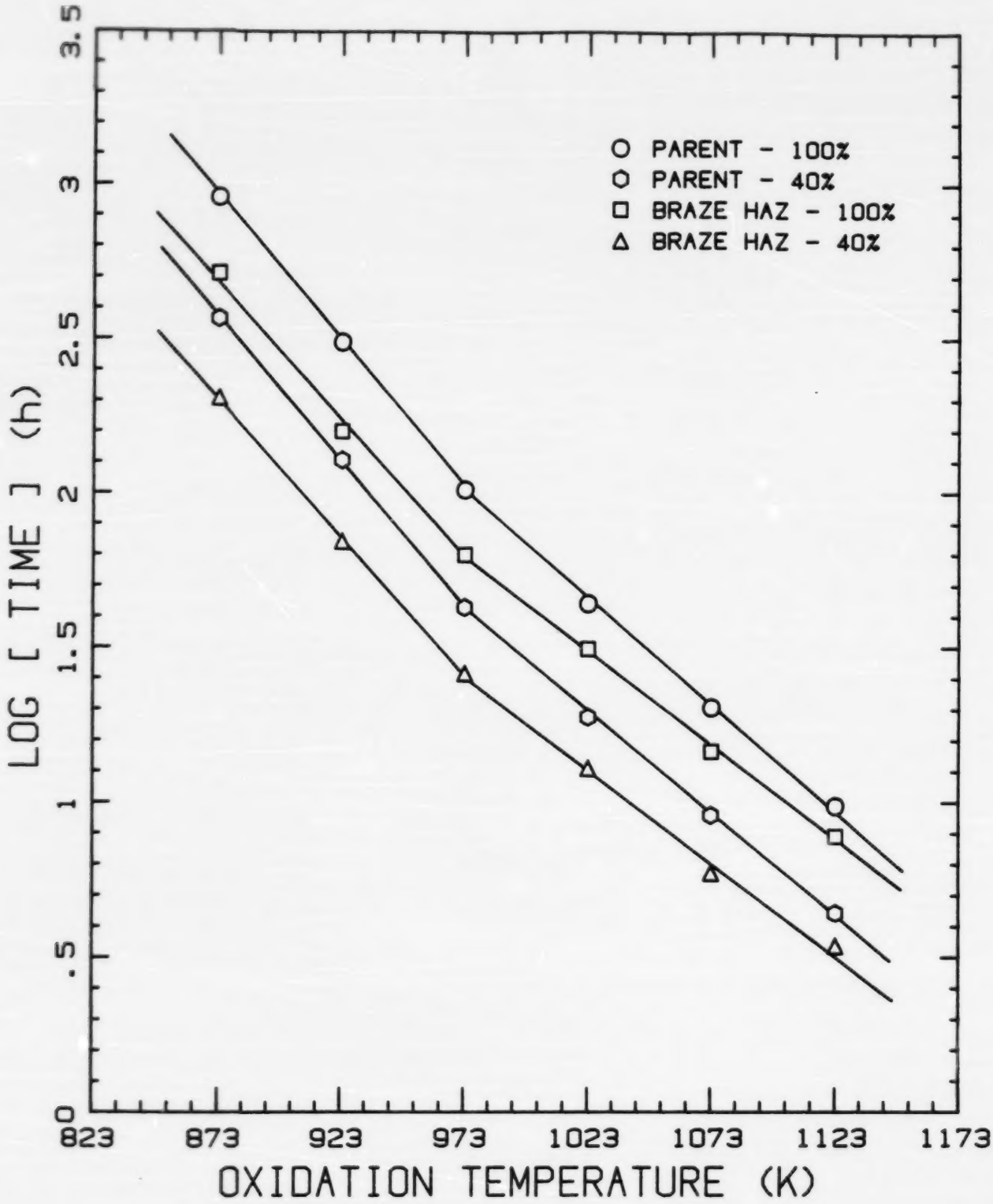

FIGURE 22: PLOTS ILLUSTRATING THE TIMES TO OXIDIZE 40% AND 100% OF THE ORIGINAL WALL OF PARENT AND BRAZE HAZ MATERIALS IN AN AIR ENVIRONMENT AS A FUNCTION OF TEMPERATURE.

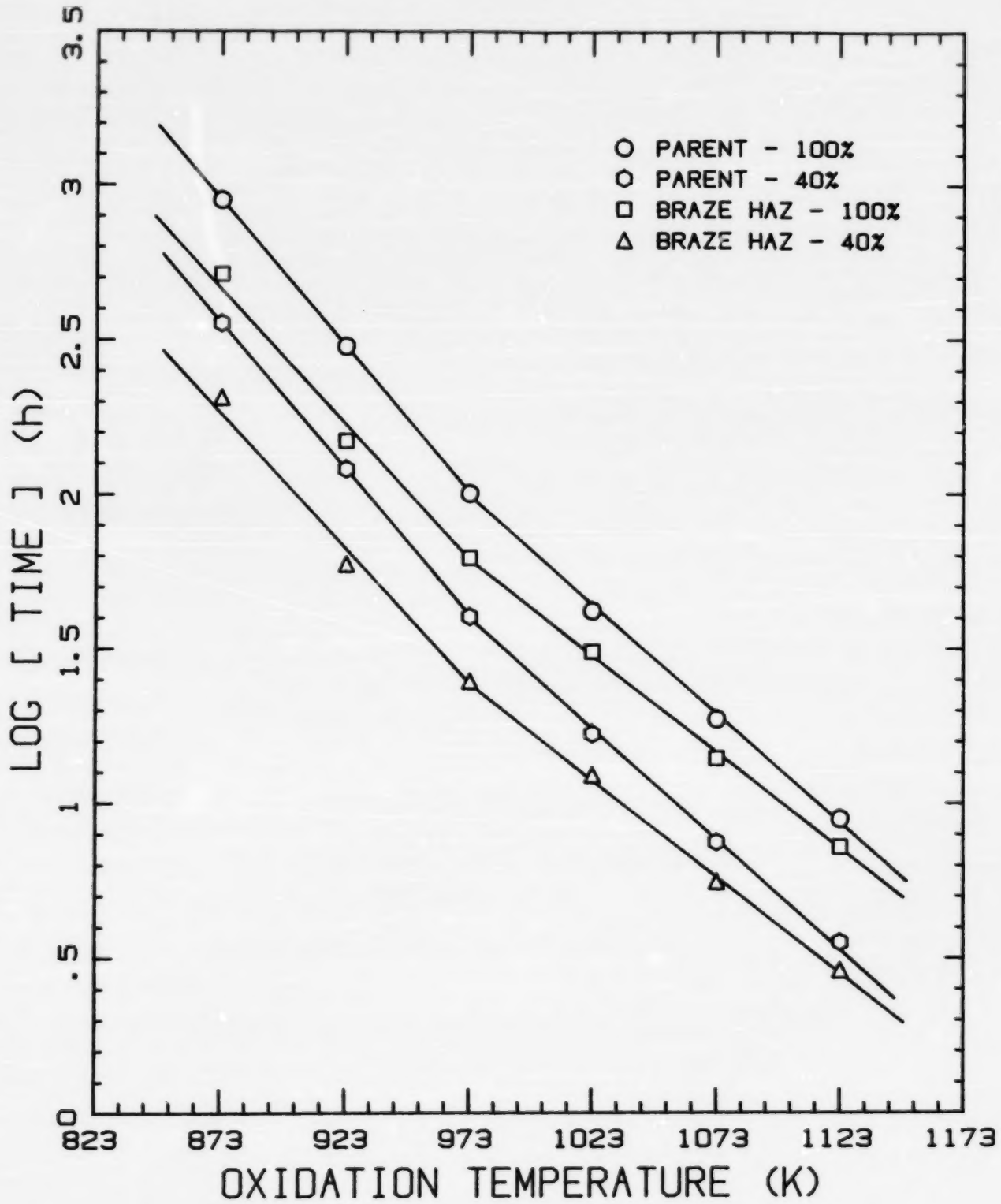

FIGURE 23: PLOTS ILLUSTRATING THE "MODIFIED" TIMES TO OXIDIZE 40% AND 100% OF THE ORIGINAL WALL OF PARENT AND BRAZE HAZ MATERIALS IN AN AIR ENVIRONMENT AS A FUNCTION OF TEMPERATURE.

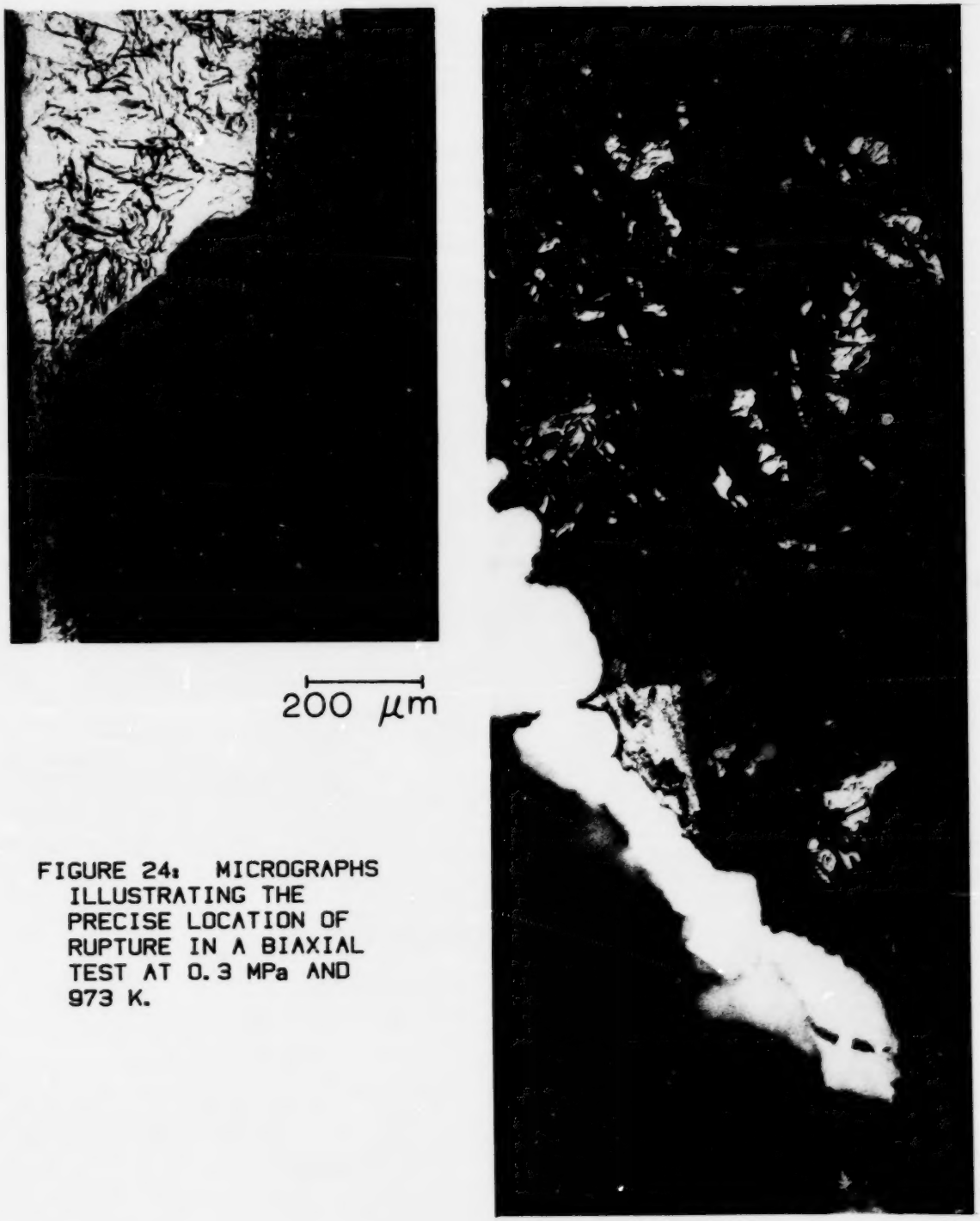

FIGURE 24: MICROGRAPHS ILLUSTRATING THE PRECISE LOCATION OF RUPTURE IN A BIAXIAL TEST AT 0.3 MPa AND 973 K.

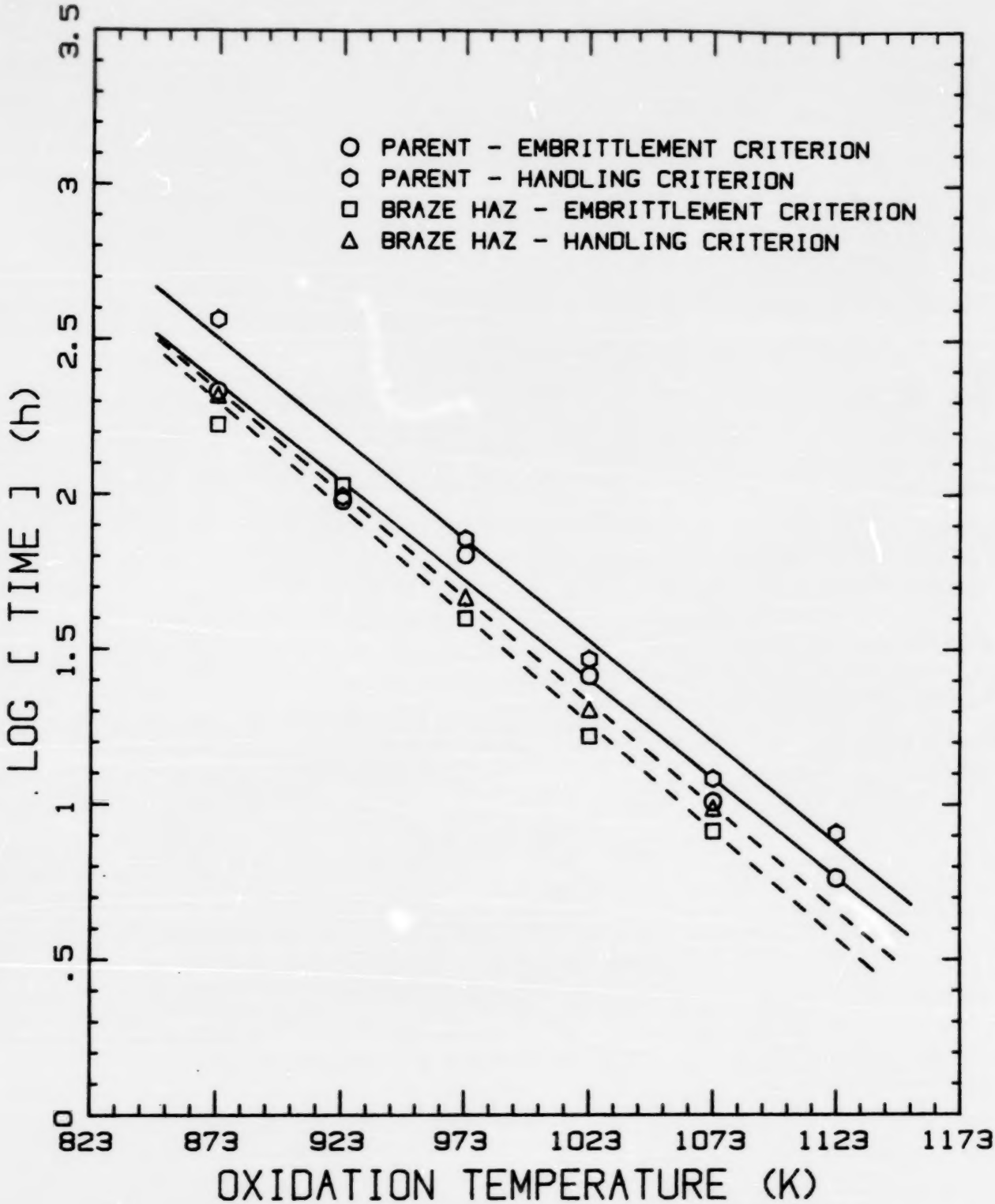

FIGURE 25: PLOTS ILLUSTRATING THE VARIATION OF THE TENTATIVE CRITERIA FOR EMBRITTLEMENT AND HANDLING OF CANDU ZIRCALOY-4 FUEL CLADDING MATERIAL IN AN AIR ENVIRONMENT AS A FUNCTION OF TEMPERATURE.

DISTRIBUTION

Dr. G. Brenciaglia	Technical & Training Services, A7C4
Dr. D. Mills	Director of Research
Dr. P.T. Truant	Technical & Training Services, A7B4
Mr. J. Novak	Technical & Training Services, A7B4
Mr. C. Blahnik	Design & Development - Gen, H11F13
Mr. J.H.K. Lau	Design & Development - Gen, H11F14
Mr. F.C. Iglesias	AECL-CRNL
Dr. H.E. Rosinger	AECL-WNRE
Mr. E.E. Merlo	AECL-CO, Sheridan Park
Dr. R. Sejnoha	AECL-CO, Sheridan Park
Mr. N. Graham	Westinghouse Canada Ltd., Port Hope
Dr. J. Brown	Metallurgical Research
Dr. R.G. Fleck	Metallurgical Research
Dr. P.C. Lichtenberger	Metallurgical Research
Dr. B. Mukherjee	Metallurgical Research
Mr. M.J. McGraw	Metallurgical Research
Mr. A. Donner	Metallurgical Research
Dr. E.T.C. Ho (2)	Metallurgical Research

Public Reference Centre
Editorial Section (2)
Office Copies (3)
Extra Copies (3)